Microbe-microbe and microbe-host interactions

The *Pseudomonas putida* T6SS is a plant warden against phytopathogens

Patricia Bernal[1,2], Luke P. Allsopp[1], Alain Filloux[1] and María A. Llamas[2]

[1]MRC Centre for Molecular Bacteriology and Infection, Department of Life Sciences, Flowers Building, 1st floor South Kensington Campus, Imperial College London, London SW7 2AZ, UK [2]Department of Environmental Protection, Estación Experimental del Zaidín-Consejo Superior de Investigaciones Científicas, 18008 Granada, Spain

Correspondence: P Bernal and A Filloux, MRC Centre for Molecular Bacteriology and Infection, Department of Life Sciences, Flowers Building, 1st floor South Kensington Campus, Imperial College London, London SW7 2AZ, UK

E-mails: p.bernal@imperial.ac.uk and a.filloux@imperial.ac.uk

Running title: *P. putida* T6SS is a biocontrol weapon

Abstract

Bacterial type VI secretion systems (T6SSs) are molecular weapons designed to deliver toxic effectors into prey cells. These nanomachines play an important role in inter-bacterial competition and provide advantages to T6SS active strains in polymicrobial environments. Here we analyse the genome of the biocontrol agent *Pseudomonas putida* KT2440 and identify three T6SS gene clusters (K1-, K2- and K3-T6SS). Besides, ten T6SS effector/immunity pairs were found, including putative nucleases and pore-forming colicins. We show that the K1-T6SS is a potent antibacterial device which secretes a toxic Rhs-type effector Tke2. Remarkably, *P. putida* eradicates a broad range of bacteria in a K1-T6SS-dependent manner, including resilient phytopathogens which demonstrates that the T6SS is instrumental to empower *P. putida* to fight against competitors. Furthermore, we observed a drastically reduced necrosis on the leaves of *Nicotiana benthamiana* during co-infection with *P. putida* and *Xanthomonas campestris*. Such protection is dependent on the activity of the *P. putida* T6SS. Many routes have been explored to develop biocontrol agents capable of manipulating the microbial composition of the rhizosphere and phyllosphere. Here we unveil a novel mechanism for plant biocontrol which needs to be considered for the selection of plant wardens whose mission is to prevent phytopathogen infections.

Introduction

The type VI secretion system (T6SS) is found in more than 25% Gram-negative bacteria and used to inject toxic proteins into prokaryotic or eukaryotic cells (Ho et al. 2013). Initially the T6SS was assigned a role in virulence and eukaryotic cell manipulation (Ma & Mekalanos 2010; Miyata et al. 2011). Further analyses showed that this system plays a key role in inter-bacterial competition (Ho et al. 2013). It provides selective advantages to producer strains by annihilating competitors either in an indiscriminate manner or in response to danger signals (Ho et al. 2013; Basler et al. 2013; Hood et al. 2010; Hachani et al. 2014). The T6SS toxins are usually produced together with immunity proteins that prevent self-intoxication. In molecular terms, the T6SS displays structural similarities with the tail and the puncturing device of the bacteriophage T4 (Cascales & Cambillau 2012; Filloux 2011; Leiman et al. 2009). It is composed by thirteen core components of which some have now been assigned clear functions (Fig. 1a). TssB and TssC form a contractile sheath that encases a tube formed by rings of Hcp hexamers (Kudryashev et al. 2015). A puncturing device made up of a trimeric VgrG spike is placed on top of the Hcp tube and crowned with a PAAR-protein (Cascales & Cambillau 2012; Shneider et al. 2013). The cytosolic part of the T6SS docks onto a membrane complex (TssLMJ) likely by interacting with a phage baseplate-like structure (Durand et al. 2015; Planamente et al. 2016; Filloux & Freemont 2016). Upon contraction of the TssBC sheath, the T6SS effectors are propelled out of the bacterium together with the Hcp and VgrG proteins and delivered into prey cells (Basler & Mekalanos 2012). Finally, the ClpV ATPase binds the contracted sheath for disassembly and recycling enabling another round of injection (Kube et al. 2014; Kapitein et al. 2013). The T6SS is usually quite modular and can accommodate different combinations of VgrG/PAAR proteins to form the tip. This modularity allows the delivery of a great variety of effectors (Shneider et al. 2013;

Hachani et al. 2014; Whitney et al. 2014). Alternatively, the effectors can also be ushered in and delivered by the tube-forming Hcp protein (Silverman et al. 2013). Thus, a wide variety of effectors with a broad range of activities can be secreted by a single T6SS. T6SS effectors have been classified into specialised and cargo effectors (Cianfanelli et al. 2016). Specialised effectors are domains, usually at the C-terminus of specific T6SS structural components that are coined as "evolved" VgrG, PAAR or Hcp proteins. In contrast, cargo effectors interact non-covalently with "canonical" VgrG, PAAR or Hcp proteins (Durand et al. 2014). Several cargo effectors carry a motif named MIX (marker for type six effectors) that is proposed to be required for recognition and direct interaction with VgrG or PAAR proteins (Salomon et al. 2014). Specific adaptors such as Tap/Tec and EagR proteins are likely to facilitate the interaction between the structural components of the T6SS tip and the effectors (Unterweger et al. 2015; Liang et al. 2015; Alcoforado Diniz & Coulthurst 2015). Finally, accessory elements (named *tag* from T6SS accessory genes) are required to modulate the assembly of the system and/or confer additional functions (Boyer et al. 2009).

The T6SS was first identified in two pathogenic bacteria, *Vibrio cholerae* and *Pseudomonas aeruginosa* (Mougous et al. 2006; Pukatzki et al. 2006) and analysed later in many other pathogens (Lin et al. 2013; Suarez et al. 2008; Murdoch et al. 2011; de Pace et al. 2010; Burtnick et al. 2011; Rosales-Reyes et al. 2012). However, analytical description of T6SS in non-pathogenic bacteria is underrepresented in the literature (Bladergroen et al. 2003; Marchi et al. 2013), despite an even distribution in both classes of organisms (Boyer et al. 2009). *Pseudomonas putida* is a saprophytic soil bacterium that has the capacity to colonise the root of crop plants (Espinosa-Urgel et al. 2000; Molina et al. 2000). It is a well-established biocontrol agent that provides growth advantages to the plant (Weller 2007). In this study we identified and characterized the

P. putida T6SS which exhibits great variety and complexity both in terms of apparatus and secreted toxins. We showed that this secretion system is used by the bacterium to drive killing of resilient phytopathogens and appears to be a major player in its biocontrol portfolio.

Materials and methods

Bacterial strains and growth conditions

Bacterial strains are listed in Table S1. *P. putida* mutants were constructed by allelic exchange as described previously (Vasseur et al. 2005). Briefly, 750-bp DNA fragments upstream and downstream the gene to be deleted were amplified using KT2440 genomic DNA. Mutator fragments were obtained by overlapping PCR, cloned into pCR-BluntII-TOPO (Invitrogen), sequenced and subcloned into the pKNG101 suicide vector (Kaniga et al. 1991). A similar approach was used to replace the wild-type *tke2* gene with *tke2*-V5 encoding a C-terminally V5-tagged Tke2 protein. The *hcp1*-HA gene encoding a C-terminal HA-tagged Hcp1 protein was introduced on the chromosome using the miniCTX transposon (Hoang et al. 2000). Insertions and gene replacements were confirmed by PCR. All strains were grown in LB (Sambrook et al. 1989). For secretion assays, tryptone soya broth (TSB) medium (Oxoid) was used. *E. coli* was incubated at 37°C, and *P. putida* and the phytopathogens at 25-30°C. Antibiotics were used at (µg ml^{-1}): ampicillin (Ap), 100; gentamycin (Gm), 20; kanamycin (Km), 50; piperacillin (Pip), 25; rifampicin (Rif), 20; streptomycin (Sm), 100; tetracycline (Tc), 50.

Plasmids and cloning

Plasmids are described in Table S1 and primers listed in Table S2. PCR amplifications were performed using Phusion® Hot Start High-Fidelity (Finnzymes), KOD Hot Start (EMD Millipore) or Taq (Roche) DNA polymerases. Recombinant plasmids were sequenced and transferred to *P. putida* by electroporation (Choi et al. 2006) or conjugation (Ramos-Gonzalez et al. 1991).

Bioinformatic analyses

Pseudomonas sequences were obtained from the Pseudomonas Genome database (Winsor et al. 2016). BLASTP analyses were performed at the NCBI website (Boratyn et al. 2013) and amino acid sequence searches using SMART (Letunic et al. 2015) and Pfam (Finn et al. 2016). The Protein Homology/analogy Recognition Engine (Phyre2) server was used to perform structural-base homology prediction (Kelley et al. 2015). The PyMOL Molecular Graphics System (Version 1.8 Schrondinger, LLC) was used to build structural alignments. The phylogenetic tree was constructed using MEGA6 (Tamura et al. 2013). PSORTb software and SOSUI GramN server were used to predict sub-cellular location of proteins (Yu et al. 2010; Imai et al. 2008), TMHMM software to predict transmembrane domains (Krogh et al. 2001), and SignalP and SOSUIsignal to predict signal peptides (Petersen et al. 2011; Gomi et al. 2004). Synteny was analysed using the CoGe's Genome Evolution tool (Lyons & Freeling 2008). The UGENE bioinformatics software was used to identify open reading frames (*orfs*) (Okonechnikov et al. 2012).

Secretion assays

Bacterial strains were grown in TSB for 5 hours at 30°C and the extracellular fraction obtained and analysed as previously described (Hachani et al. 2011). The proteins in the

culture supernatants were precipitated with trichloroacetic (TCA) acid and resuspended in 1M of Tris-base and 4x Laemmli buffer. Proteins were separated by SDS-PAGE containing 8% or 15% (w/v) acrylamide and electro-transferred to nitrocellulose membranes. Immunodetection was performed using monoclonal antibodies directed against the influenza hemagglutinin (HA) epitope (HA.11, Covance) or the paramyxovirus of simian virus 5 (V5) epitope (Invitrogen). A monoclonal antibody against the β subunit of the RNA polymerase (Neoclone) was also used. The secondary antibody, horseradish peroxidase-conjugated rabbit anti-mouse (Sigma), was detected using the SuperSignal® West Pico Chemiluminescent Substrate (Thermo Scientific). Blots were scanned and analysed using the Image Reader LAS-3000 (Fuji).

Growth inhibition assays

Overnight LB cultures of *E. coli* DH5α harbouring the vectors pNDM220 (Gotfredsen & Gerdes 1998), pBAD33 (Guzman et al. 1995) or derivatives encoding Tke2 or Tki2 were adjusted to OD_{600} of 0.1. Expression of *tke2* and *tki2* was induced with 0.2% (w/v) L-arabinose and 1 mM isopropyl β-D-1-thiogalactopyranoside (IPTG), respectively.

Interbacterial competition assays

In vitro competition assays were performed on LB plates as previously described (Hachani et al. 2013). Bacterial overnight cultures were adjusted to OD_{600} of 1 in PBS and mixed in a 1:1 ratio (*P. putida*-prey). Bacteria were co-cultured at 30°C for 5 hours (*E. coli*) or 24 hours (phytopathogens). The competition was quantified by counting colony forming units (CFU) upon antibiotic selection. At least three biologically independent experiments were performed. *In planta* competition assays were carried out by infiltration of bacteria into *Nicotiana benthamiana* leaves as described before (Ma et

al. 2014). Overnight cultures of *P. putida* and *X. campestris* were adjusted to OD_{600} of 0.01 in PBS and mixed in a 1:1 ratio. Approximately 100 µl volume was infiltrated on the reverse of a 1 month-old leaf and the infiltration area marked. After 24 hours of incubation in a plant chamber (23°C, 16 hours-light) CFUs were determined. A section of the leaf from the infiltration area was cut out, homogenised in PBS and subsequently serially diluted. The leaves were visualized by fluorescence microscopy using a Leica M206FA stereomicroscope. Imaging was performed at room temperature with a 1x objective. The evaluation of necrosis was based on the coloration of the leaves following previous standard evaluation of virulence that goes from no visible effects to changes in the tissue colour of the leaf, which can shift from green to yellowish (chlorosis), yellowish to brownish and blackening of the leaf (necrosis), up to complete rotting of the leaf at later stages (Katzen et al. 1998). In our assay the circled zones point at deep brown colour area."

Results

Genome wide screening for T6SSs in P. putida *species*

In silico analyses of forty *P. putida* strains revealed that all encode T6SS genes and 90% of them have at least one cluster encoding a full set of T6SS components (Table S3). The number of T6SS clusters in a single strain ranged from zero in *P. putida* BIRD-1 or H8234 to four in *P. putida* PA14H7, while most strains contained one or two clusters (Table S3). In total, we identified sixty-six complete T6SS gene clusters distributed in three main phylogenetic clades (Fig. 2). Following previous nomenclature (Boyer et al. 2009; Barret et al. 2011) we referred to these three groups as 1.2, 2 and 4B. Eighty percent of the clusters belong to group 1.2 or 4B, whereas 10% are found in group 2 (Fig. 2). Each of

these groups contains distinguishable genetic architecture and features (Figure S1), as described in the next section.

The reference strain P. putida *KT2440 is equipped with three T6SSs*

We used the strain KT2440 to perform in depth genomic analysis. In this strain, only five T6SS-related genes, *i.e.* the *hcp* genes PP2615 and PP4082 or the *vgrG* genes PP2614, PP3386 and PP4049 are annotated (http://pseudomonas.com/). Using bioinformatics approaches (*e.g.* BLASTP, Ugene or SMART) we identified a large number of T6SS-related *orf*s (Tables S4-S6). Most of the genes fall into three clusters that we named K1-, K2- and K3-T6SS (Fig. 1b,c,d, Tables S4-S5). Several *hcp* and *vgrG* orphan genes were also found scattered on the chromosome (Fig. 1b,e and Table S6). Phylogenetic analysis showed that the K2- and K3-T6SSs are related (group 1.2, Fig. 2) whereas the K1 cluster clades separately (group 4B, Fig. 2).

K2 and K3 consist of two divergently transcribed gene clusters that contain 12 of the 13 genes encoding core T6SS components (Fig. 1d). The missing core gene, *clpV*, encodes the ATPase required for disassembling the sheath (Kube et al. 2014; Kapitein et al. 2013), which is absent in all clusters belonging to group 1.2 (data not shown). Using the "CoGe's Genome Evolution Analysis" tool we observed a synteny among the K2 and K3 clusters (Fig. 1d). The identity of the corresponding proteins encoded within each of these clusters was remarkably high, ranging from 64 to 99% (Table S5). These observations indicate that the two clusters may have arisen from a duplication event.

The K1 system is not related to K2 and K3 and belongs to the plant-related group (group 4B, Fig. 2) (Boyer et al. 2009). This cluster comprises two putative operons and an "intermediate" region (Fig. 1c). The first operon contains 15 genes, 12 of which encode T6SS core components, and was named the structural operon (Fig. 1c). The last core

component gene, *vgrG*, is located within the second operon that was therefore named the VgrG1 operon (Fig. 1c). Within the structural operon we found a previously undefined *orf*, PP3090.1 encoding the accessory protein TagF1 (Table S4). An orthologue of this protein was reported to function as a post-transcriptional regulator (Silverman et al. 2011). Another accessory gene encodes TagP1 (Table S4), a TssM derivative whose C-terminal periplasmic portion carries a peptydoglycan binding domain (pfam00691) (Aschtgen et al. 2010). Finally, our analysis identified a novel T6SS feature represented by the first gene in the K1-T6SS structural operon, PP3100.1, *tagX1* (Fig. 1c and Table S4). The protein encoded by this gene has no homologues or recognizable features. It has not been assigned a role in the T6SS but is exclusively present in all clusters belonging to the 4B group (*i.e. P. putida* and *Pseudomonas syringae*).

The K1-T6SS is functional and anti-bacterial

Hcp release is dependent on the T6SS and is a reliable marker for assessing functionality of the system (Pukatzki et al. 2006). Therefore, we engineered *P. putida* strains producing an HA-tagged version of Hcp1 to assess K1-T6SS activity. TssA is a core baseplate component of the T6SS, is essential for T6SS activity (Planamente et al. 2016) and we used a *tssA* mutant to disable the *P. putida* T6SSs. We readily detected Hcp1 in the supernatant of wild-type cultures but not in an isogenic *tssA1* mutant (Fig. 3a), thus establishing that the K1-T6SS is a functional secretion machine.

Several characterized T6SSs have anti-bacterial activity, resulting from the injection of T6SS toxins into bacterial preys (Russell et al. 2014; Cianfanelli et al. 2016). We performed competition assays using *E. coli* K12 as prey and *P. putida* wild-type or T6SS mutants as predators. The *E. coli* prey harbours a plasmid that confers blue colour to the colony in the presence of X-gal (Fig. 3b). In a mixed culture, the *P. putida* wild-type

strain was able to annihilate *E. coli*, whereas mutants in any of the K1-T6SS structural genes (*tssA1*, *tssL1*, *tssK1*, *tssG1*, *tssF1* or *tssE1*) were no longer outcompeting *E. coli* (Fig. 3b). In contrast, mutants in the K2- or K3-T6SS clusters, *P. putida* Δ*tssM2* and Δ*tssM3*, respectively, still efficiently annihilated *E. coli* (data not shown). We concluded that K1 is the most active KT2440 T6SS *in vitro*, as under the laboratory conditions used here, and that its antibacterial activity may result from the secretion of T6SS effectors.

P. putida *KT2440 encodes a wealth of T6SS bacterial effectors*

Genes encoding putative T6SS effectors and cognate immunity proteins (EI pairs) are often linked to *hcp*, *vgrG* genes and/or genes encoding chaperones/adaptors (Dong et al. 2013; Liang et al. 2015; Unterweger et al. 2015; Ma et al. 2014; Hachani et al. 2014). Our *in silico* analyses identified a total of ten potential EI pairs most of them encoded in the vicinity of *vgrG*/*hcp* genes and in some cases near genes encoding Tap or EagR adaptors (Fig. 1c-e and Tables S4-S6). These EI pairs have been named Tke and Tki for Type six KT2440 effector and immunity, respectively (Fig. 4a).

VgrG linked effectors

Downstream *vgrG1* and *vgrG2* in the K1 and K2 clusters, respectively, putative effector genes, *tke2* and *tke4*, and EagR adaptor genes, *eagR1a-eagR1b* and *eagR2*, were found (Fig. 1c-d). Tke2 and Tke4 proteins share a similar structure, both containing an N-terminal PAAR motif (Cascales & Cambillau 2012; Shneider et al. 2013) and a conserved Rhs domain (Busby et al. 2013) limited by specific RVxxxxxxxxG and PxxxxDPxGL motifs (Fig. 4 a-b). PAAR proteins have been shown to be located at the tip of the VgrG trimer, sharpening the T6SS spike and/or creating an interface for T6SS effectors and adaptors (Whitney et al. 2015). The C-terminal region of Tke2 or Tke4 (110 and 102 amino acid-long, respectively) carries a cytotoxic domain. This domain is similar in both

proteins and belongs to the HNH superfamily of nucleases *e.g.* colicin E7 and pyocin S1 (Fig. 4a and 5a) (Huang & Yuan 2007) although Tke4 domain contains a specific SHH signature (Fig. 4a and 5b). Genes encoding putative effectors were also found downstream *vgrG3*, *vgrG4* and *vgrG5* (Fig. 1d-e). The *tke5* and *tke9* genes within the K3 and *vgrG4* operons, respectively, are linked to genes encoding Tap adaptors (*tap3* and *tap4*) (Fig. 1d-e). No recognizable features were found in Tke5 or Tke9, except for a conserved N-terminal MIX motif considered a marker for T6SS effectors (Salomon et al. 2014) (Fig. 4a, and 4c). This motif is also present in the effector encoded downstream *vgrG5*, Tke10, which is predicted to be a restriction endonuclease (REase) (Fig. 1e and Fig. 4c). In addition, *tke5* and *tke10* are linked to genes encoding a PAAR-motif (named *tsp* for *type six paar*) (*tsp5* and *tsp10*) (Fig. 1d-e, 4b and Table S6).

Effectors encoded in proximity to *hcp* genes

The potential effector genes *tke6*, *tke7* and *tke8* were found within or in the vicinity of the three *hcp* orphan operons (*hcp4*, *hcp5* and *hcp6*) (Fig. 1e and Table S6). These effectors have similarities with pore-forming colicins (*i.e.* colicin S4) (Fig. 4a, 5c and Table S6). The *tke6, tke7* and *tke8* genes are not genetically associated with *vgrG* or T6SS adaptor genes. These *hcp*-linked T6SS effectors could be delivered by docking into the lumen of the Hcp ring, instead of being attached at the VgrG tip, as observed with the *P. aeruginosa* Tse2 effector (Silverman et al. 2013). In contrast to *tke7* and *tke8*, *tke6* is not located within the *hcp* operon but 5 kb upstream of the *hcp4* gene. Interestingly, *hcp4* has a premature stop codon and might not be functional (Fig. 1e and Table S6) while Tke6 has an N-terminal PAAR domain (Fig. 4a-b). Thus, in contrast to Tke7 and Tke8 that lack PAAR or MIX domains, the delivery of Tke6 could be mediated by a VgrG protein through a PAAR-VgrG interaction.

Orphan effectors

We found two additional potential EI pairs (*tke1-tki1* and *tke3-tki3*) within the K1-T6SS cluster both lacking PAAR or MIX motifs. Tke1 is an orthologue of the *P. aeruginosa* Tse6 which presents a C-terminal region carrying a toxic domain known as Toxin_61 (Fig. 4a and S2a) (Hachani et al. 2014; Whitney et al. 2014) and degrades NAD(P)(+) in target cells (Whitney et al. 2015). In case of Tke3, a Phyre2 analysis suggests that the C-terminal domain resembles the B30.2 fragment from the human protein TRIM20 (Weinert et al. 2015) (Fig. S2b and Table S5).

In summary, we identified ten potential T6SS effectors in the KT2440 genome. Three of them Tke2, Tke4 and Tke6 have an N-terminal PAAR-domain (Fig. 4a-b) and are therefore considered "specialised" effectors. The others are not fused to any T6SS component and their domain architecture suggests they are "cargo" effectors.

Tke2/Tki2 is a P. putida *K1-T6SS effector/immunity pair*

We have shown that the K1 system is functional and that the corresponding gene cluster encodes several EI pairs including Tke2/Tki2 (Fig. 1c, 4a, 5a and Table S4). To assess the functionality of this EI pair, the *tke2* and *tki2* genes were cloned into compatible plasmids and transformed into *E. coli* K12. Expression was induced by the addition of IPTG (*tke2*) or arabinose (*tki2*). Upon induction of the effector gene *tke2*, *E. coli* growth was significantly impaired (Fig. 6a-b) but growth could readily be rescued upon co-expression of the putative Tki2 immunity protein (Fig. 6a-b). This suggests that Tke2/Tki2 is a genuine EI pair.

We assessed whether Tke2 is secreted in a K1-T6SS-dependent manner. The corresponding gene was replaced on the KT2440 chromosome with a version encoding a C-terminally V5-tagged protein. However, Tke2-V5 production was only weakly

detected when using this strain (Fig. S3). In contrast to bacterial killing which is a highly sensitive assay, detection of secreted T6SS toxins by western-blot may need higher level of T6SS expression (Cianfanelli, et al. 2016). It has been described in other bacteria that several global regulators are involved in T6SS expression, including the alternative sigma factor RpoN (Bernard et al. 2010, 2011; Sana et al. 2013). The *tke2-V5* chimeric gene was introduced into an *rpoN* mutant and in this strain Tke2 production was considerably increased as compared to the wild-type *P. putida* (Fig. S3). We thus used this genetic background to analyse Tke2 secretion. Tke2 was produced in both the *rpoN* strain and the isogenic T6SS mutant (*rpoNΔtssA1*), but was only found in the supernatant of the strain with an intact T6SS (Fig. 6c). Our results show that Tke2 is an effector of the K1-T6SS and its activity is antagonized by the Tki2 immunity protein.

P. putida *outcompetes plant pathogens in a T6SS-dependent manner*

P. putida is an efficient biocontrol agent (Amer & Utkhede 2000; Validov et al. 2007), and we hypothesized that it uses the T6SS to kill ecologically-relevant competitors. To test this we selected four plant pathogens, *P. syringae*, *Xanthomonas campestris*, *Pectobacterium carotovorum* and *Agrobacterium tumefaciens*, that are leading causes of deadly diseases in several economically-important crops (Mansfield et al. 2012). The various T6SSs are likely to be differentially expressed *in vitro, in vivo, in planta* or in the presence of different competitors (Ma et al. 2014). In order to assess whether the T6SS in general is required for outcompeting plant pathogens and thus involve in plant protection we used a triple T6SS mutant (Δ*tssA1*Δ*tssM2*Δ*tssM3*, also named ΔT6SS) so that none of the K1, K2 or K3 system is at play. First, a competition assay between KT2440 or the triple mutant, and the phytopathogens was performed. The *P. putida* wild-type strain caused a 10-fold decrease in survival of *A. tumefaciens* and *P. caratovorum*

and a 1000-fold decrease in the survival of *X. campestris* and *P. syringae* (Fig. 7). The *P. putida* T6SS mutant had barely any impact on the survival of any of these bacteria (Fig. 7). Our results indicate that KT2440 outcompetes all challenged phytopathogens in a T6SS-dependent manner and suggest a role for this secretion system in biocontrol.

T6SS-active P. putida *protects plants from pathogen's attack*

To assess the ability of *P. putida* to kill phytopathogens in an ecologically-relevant set-up we developed an *in planta* competition assay. We selected *X. campestris* as the pathogen and *Nicotiana benthamiana* as the plant model. Leaves were co-infected with *X. campestris* and either *P. putida* wild-type or the isogenic ΔT6SS mutant. *X. campestris* was tagged with a green-fluorescent protein to monitor *in situ* colonisation. *X. campestris*-induced halos of necrosis on the leaves were observed 5 days post-infection, whereas inoculation with *P. putida* resulted in healthy-looking leaves (Fig. 8a). Remarkably, co-infiltration of *X. campestris* and *P. putida* wild-type strain considerably reduced the necrotic areas produced by *X. campestris* (circled in Fig. 8b). This is not observable with the *P. putida* ΔT6SS mutant and we concluded that interference with *X. campestris* colonisation is T6SS dependent (Fig. 8b). The protection conferred by *P. putida* is due to reduced survival of *X. campestris* in the leaves (~2.5-fold reduction), as qualitatively observed by fluorescence microscopy (Fig. 8b) and quantitatively measured by CFU counting (Fig. 8c). Our results show that *P. putida* outcompetes *X. campestris* during plant colonization and this process involves the bactericidal properties of the T6SS.

Discussion

The type VI secretion system was discovered in the bacterial pathogens *V. cholerae* (Pukatzki et al. 2006) and *P. aeruginosa* (Mougous et al. 2006). Since then an increasing

number of studies has provided details on the function and structure of this original bacterial secretion system (Hachani et al. 2016; Russell et al. 2014; Zoued et al. 2014; Cianfanelli, et al. 2016). However, although the presence of the T6SS in non-pathogenic strains is evident (Boyer et al. 2009), little work has been done to understand its relevance in this category of bacteria (Bladergroen et al. 2003; Mougous et al. 2006; Pukatzki et al. 2006; Aschtgen et al. 2008).

Phylogeny and genetic structure of the P. putida *T6SS clusters.* In this study we have identified a total of 66 T6SS clusters among *P. putida* strains, which suggests that this secretion machine plays an important role in *P. putida* physiology and fitness. The *P. putida* T6SS clusters clade within three phylogenetic groups, group 1.2, 2 or 4B (Fig. 2). Remarkably, *P. putida* is the only *Pseudomonas* species encoding T6SSs from group 1.2, while T6SSs from group 4B are only present in *P. putida* and *P. syringae* (Barret et al. 2011). The *P. putida* KT2440 strain contains two clusters from group 1.2 (K2 and K3) and one cluster from group 4B (K1). The K2-T6SS cluster contains two *orf*s, *vgrG2* and *tssC2*, that present premature stop codons (Table S5) implying that this system is not functional. Prematurely interrupted T6SS genes have been identified in functional T6SSs of *Citrobacter rodentium* and *Yersinia pseudotuberculosis* (Gueguen et al. 2014). In these cases, a transcriptional frame-shifting caused by a poly-A tract allows the production of functional TssM variants (Gueguen et al. 2014). However, this is unlikely to be the case in KT2440 since poly-A tracts are not found either in *tssC2* or in *vgrG2*. Alternatively, related VgrGs (*i.e.* VgrG3, VgrG4 and VgrG5) (Fig. S4) and TssC proteins (*i.e.* TssC3) (Table S5) could be shared between different T6SSs.

The K2 and K3 clusters do not encode a ClpV protein, the ATPase responsible for disassembling the T6SS sheath. Yet, orphan *clpV* genes can be used. There are three Clp ATPase-encoding genes in the KT2440 genome (*i.e.* PP0625, PP3316 and PP4008), but

none encodes a protein from the ClpV family (Fig. S5). They are ClpA and ClpB members, which are phylogenetically distant from ClpV (Schlieker et al. 2005). Alternatively, the ClpV1 component within the K1 cluster could be shared between the systems but possibly a ClpV component may not be necessary for the function of the group 1.2 T6SS, as some *P. putida* strains (*i.e.* S12, B001, SJ3 and S610) exclusively contain a group 1.2 cluster (Table S3). In fact, functional T6SSs lacking the *clpV* gene have been identified in other bacteria (Chow & Mazmanian 2010; Bröms et al. 2012). Furthermore, the *clpV* gene of *V. cholerae* can be deleted without a total loss of T6SS function (Zheng et al. 2011). After all, other nanomachines structurally comparable to the T6SS such as the contractile-tailed phages or R-type pyocins, do not use a ClpV homolog for their function. Instead, recently discovered phage-like protein translocation structures (PTLS), are encoded within gene clusters that also carry a *clpV* homologue (Kube & Wendler 2015). This type of structure may have evolved divergently with the some T6SS subgroups and acquired ClpV from ancestral systems.

Antibacterial activity of the P. putida *KT2440 T6SS.* The main role of the T6SS is to inject effectors into eukaryotic or prokaryotic prey cells (Alcoforado Diniz et al. 2015; Hachani et al. 2016). We identified an impressive battery of ten potential T6SS effectors in *P. putida* KT2440. This is not unique but suggests that *P. putida* is primed to fight a wide range of competing organisms. At least three effector-immunity (EI) pairs are encoded within the K1-T6SS cluster (i.e. *tke1-tki1*, *tke2-tki2* and *tke3-tki3*), which belongs to the uncharacterized plant-related group (group 4B, Fig. 2). A remarkable characteristic of the system is the presence of a conserved accessory gene, *tagX*, systematically absent from other T6SS groups and which is a hallmark for group 4B systems. Here we show that suitable preys for the K1-T6SS are bacterial cells and that the Tke2 toxin contributes to the antibacterial activity. Tke2 contains a canonical Rhs-effector domain organisation,

which includes an N-terminal PAAR motif, a central domain of conserved Rhs-repeats, and a C-terminal toxic domain. Although the function of the Rhs domain is still unknown, it has been suggested that it forms a shell structure that encapsulates the C-terminal region of effectors (Busby et al. 2013) (Fig. S6). Furthermore, a specific adaptor named EagR (named after "Effector-associated gene") that contains the DUF1795 domain, has been involved in the secretion of PAAR/Rhs-effectors (Alcoforado Diniz & Coulthurst 2015). Two different proteins containing DUF1795 domains are encoded immediately upstream *tke2* (*eagR1a* and *eagR1b*, Fig. 1c). Although the function of these adaptors has not been analysed yet, it is possible that both function together to assist Tke2 secretion. The recurrent association between PAAR/Rhs-effectors and EagR adaptors is furthermore confirmed by the association of *tke4*, encoding another *P. putida* PAAR/Rhs-effector (Fig. 1c, 4a and S6), with an *eagR* gene (*eagR2*).

Biocontrol properties of the P. putida *T6SS.* It is becoming increasingly obvious that the antimicrobial properties of the T6SS could be instrumental for the control of polymicrobial populations in excluding foes from natural and ecologically relevant environments. For instance, a clear correlation between activation of T6SS, enhanced fitness and subsequent antagonism against other bacteria has been observed with *Vibrio parahaemolyticus* in marine niches (Salomon et al. 2013). This suggested that T6SSs are key for survival and persistence of specialised species in specific habitats. In the lungs of cystic fibrosis (CF) patients, *P. aeruginosa* can persist for years while the diversity of species that primarily colonises this environment decreases over time (Marshall et al. 2015). *P. aeruginosa* isolates from CF patients have highly active T6SSs (Mougous et al. 2006; Moscoso et al. 2011), which suggests that T6SSs contribute to the colonisation advantage of *P. aeruginosa* over other species. In agreement with these observations, the T6SS has been proposed to be crucial in the establishment/evolution of the gut

microbiome (Russell, Peterson, et al. 2014; Cianfanelli, Monlezun, et al. 2016). Half of the human-associated Bacteroidetes, the dominant phyla in the human gut, not only encode T6SSs (Coyne et al. 2016) and possess a wide range of T6SS effectors but accumulate immunity genes against other T6SS effectors (Wexler et al. 2016). This strongly supports that T6SS is a selective mechanism involved in the establishment of gut communities. These remarkable properties of the T6SS are obviously useful in the development of biocontrol strains. The T6SS was originally discovered in *Rhizobium leguminosarum* and involved in pea nodulation (Bladergroen et al. 2003), but barely any studies have demonstrated the potential that such system may have in the context of the plant microbiome. A parallel can be made between the gut and the rhizosphere as both are eukaryotic based environments hosting a symbiotic relationship with a complex microbial community (Stone 2016). Both animals and plants depend on their microbiome to protect themselves against pathogens and to help assimilate necessary nutrients (Haney & Ausubel 2015; Haney et al. 2015; Carmody et al. 2015). As a defence strategy, many plant species promote the development of a specific microbiome in the rhizosphere which has antagonistic activity against soil-borne pathogens (Cook et al. 1995; Weller et al. 2002; Lebeis et al. 2015). Whilst the mechanisms for pathogen suppression are not completely understood they include the production of bioactive metabolites such as antibiotics, bacteriocins and siderophores (Weller 2007). However, these mechanisms fail to account for the full level of protection conferred by the biocontrol organism (Matilla et al. 2010). Here, we report for the first time, that the T6SS might be a primary mechanism for phytopathogen control. Indeed, we demonstrate that the crop protection agent *P. putida* KT2440 readily outcompetes a panel of economically important phytopathogens and that the efficient destruction of the pest is mostly T6SS-dependent. This property can likely be transferred to the field since this effect was observed *in vitro*

but also *in vivo* by demonstrating that *P. putida* protects plant leaves from the deleterious effect of *X. campestris*.

In our study we have used a laboratory setup and further trials in crop plants are needed so that in depth investigation of the impact of KT2440 in the rhizosphere can be assessed. Nevertheless, our finding shows that the T6SS can be used by environmental strains to protect plants from the attack of bacterial pathogens and can thus be considered as a plant health warden. This opens new possibilities in the selection of biocontrol agents used for biotechnological applications. Noticeably, the poor specificity of the T6SS (Hood et al. 2010) may allow such biocontrol organism to also fight eukaryotic pathogens belonging to different kingdoms including nematodes and fungi.

Acknowledgements

We thank Milagros Lopez (IVIA, Spain) for providing *Xanthomonas campestris* and *Pectobacterium carotovorum*, Martin Buck (Imperial College London, UK) for *Pseudomonas syringae* and Ehr Min Lai (Academia Sinica, Taiwan) for *Agrobacterium tumefaciens*. We thank Tom Wood for kindly provided the T6SS scheme shown in Fig. 1a. PB is supported by the Spanish Ministry of Economy through Juan de la Cierva grant (JCI-2010-06615), by the Andalusian Knowledge Agency through a Talent Hub grant (TAHUB-010), and by an EMBO-short term fellowship. MAL is supported by the Spanish Ministry of Economy through a Ramon&Cajal grant (RYC2011-08874). AF is supported by a BBSRC grant (BB/N002539/1).

Conflict of interest

We have no conflict of interest to disclose

References

Alcoforado Diniz J, Coulthurst SJ. (2015). Intraspecies Competition in Serratia marcescens Is Mediated by Type VI-Secreted Rhs Effectors and a Conserved Effector-Associated Accessory Protein. J. Bacteriol. 197:2350–60.

Alcoforado Diniz J, Liu Y-CC, Coulthurst SJ. (2015). Molecular weaponry: diverse effectors delivered by the Type VI secretion system. Cell. Microbiol. 17:1742–51.

Altindis E, Dong T, Catalano C, Mekalanos J. (2015). Secretome analysis of Vibrio cholerae type VI secretion system reveals a new effector-immunity pair. MBio 6:e00075.

Amer GA, Utkhede RS. (2000). Development of formulations of biological agents for management of root rot of lettuce and cucumber. Can. J. Microbiol. 46:809–16.

Aschtgen M-SS, Bernard CS, De Bentzmann S, Lloubès R, Cascales E. (2008). SciN is an outer membrane lipoprotein required for type VI secretion in enteroaggregative Escherichia coli. J. Bacteriol. 190:7523–31.

Aschtgen M-SS, Thomas MS, Cascales E. (2010). Anchoring the type VI secretion system to the peptidoglycan: TssL, TagL, TagP... what else? Virulence 1:535–40.

Barret M, Egan F, Fargier E, Morrissey JP, O'Gara F. (2011). Genomic analysis of the type VI secretion systems in Pseudomonas spp.: novel clusters and putative effectors uncovered. Microbiology (Reading, Engl.) 157:1726–39.

Basler M, Ho BT, Mekalanos JJ. (2013). Tit-for-tat: type VI secretion system counterattack during bacterial cell-cell interactions. Cell 152:884–94.

Basler M, Mekalanos JJ. (2012). Type 6 secretion dynamics within and between bacterial cells. Science 337:815.

Bernard CS, Brunet YR, Gavioli M, Lloubès R, Cascales E. (2011). Regulation of type VI secretion gene clusters by sigma54 and cognate enhancer binding proteins. J. Bacteriol. 193:2158–67.

Bernard CS, Brunet YR, Gueguen E, Cascales E. (2010). Nooks and crannies in type VI secretion regulation. J. Bacteriol. 192:3850–60.

Bladergroen MR, Badelt K, Spaink HP. (2003). Infection-blocking genes of a symbiotic Rhizobium leguminosarum strain that are involved in temperature-dependent protein secretion. Mol. Plant Microbe Interact. 16:53–64.

519 Boratyn GM, Camacho C, Cooper PS, Coulouris G, Fong A, Ma N, et al. (2013). BLAST:
520 a more efficient report with usability improvements. Nucleic Acids Res. 41:W29–33.

521 Boyer F, Fichant G, Berthod J, Vandenbrouck Y, Attree I. (2009). Dissecting the bacterial
522 type VI secretion system by a genome wide in silico analysis: what can be learned from
523 available microbial genomic resources? BMC Genomics 10:104.

524 Bröms JE, Meyer L, Sun K, Lavander M, Sjöstedt A. (2012). Unique substrates secreted
525 by the type VI secretion system of Francisella tularensis during intramacrophage
526 infection. PLoS ONE 7:e50473.

527 Burtnick MN, Brett PJ, Harding SV, Ngugi SA, Ribot WJ, Chantratita N, et al. (2011).
528 The cluster 1 type VI secretion system is a major virulence determinant in Burkholderia
529 pseudomallei. Infect. Immun. 79:1512–25.

530 Busby JN, Panjikar S, Landsberg MJ, Hurst MR, Lott JS. (2013). The BC component of
531 ABC toxins is an RHS-repeat-containing protein encapsulation device. Nature 501:547–
532 50.

533 Carmody RN, Gerber GK, Luevano JM, Gatti DM, Somes L, Svenson KL, et al. (2015).
534 Diet dominates host genotype in shaping the murine gut microbiota. Cell Host Microbe
535 17:72–84.

536 Cascales E, Cambillau C. (2012). Structural biology of type VI secretion systems. Philos.
537 Trans. R. Soc. Lond., B, Biol. Sci. 367:1102–11.

538 Chatzidaki-Livanis M, Geva-Zatorsky N, Comstock LE. (2016). Bacteroides fragilis type
539 VI secretion systems use novel effector and immunity proteins to antagonize human gut
540 Bacteroidales species. Proceedings of the National Academy of Sciences of the United
541 States of America 113:3627–32.

542 Choi K-HH, Kumar A, Schweizer HP. (2006). A 10-min method for preparation of highly
543 electrocompetent Pseudomonas aeruginosa cells: application for DNA fragment transfer
544 between chromosomes and plasmid transformation. J. Microbiol. Methods 64:391–7.

545 Chow J, Mazmanian SK. (2010). A pathobiont of the microbiota balances host
546 colonization and intestinal inflammation. Cell Host Microbe 7:265–76.

547 Cianfanelli FR, Alcoforado Diniz J, Guo M, De Cesare V, Trost M, Coulthurst SJ. (2016).
548 VgrG and PAAR Proteins Define Distinct Versions of a Functional Type VI Secretion
549 System. PLoS Pathog. 12:e1005735.

Cianfanelli FR, Monlezun L, Coulthurst SJ. (2016). Aim, Load, Fire: The Type VI Secretion System, a Bacterial Nanoweapon. Trends Microbiol. 24:51–62.

Cook RJ, Thomashow LS, Weller DM, Fujimoto D, Mazzola M, Bangera G, et al. (1995). Molecular mechanisms of defense by rhizobacteria against root disease. Proc. Natl. Acad. Sci. U.S.A. 92:4197–201.

Coyne MJ, Roelofs KG, Comstock LE. (2016). Type VI secretion systems of human gut Bacteroidales segregate into three genetic architectures, two of which are contained on mobile genetic elements. BMC Genomics 17:58.

Coyne MJ, Zitomersky NL, McGuire AM, Earl AM, Comstock LE. (2014). Evidence of extensive DNA transfer between bacteroidales species within the human gut. MBio 5:e01305–14.

Dong TG, Ho BT, Yoder-Himes DR, Mekalanos JJ. (2013). Identification of T6SS-dependent effector and immunity proteins by Tn-seq in Vibrio cholerae. Proc. Natl. Acad. Sci. U.S.A. 110:2623–8.

Durand E, Cambillau C, Cascales E, Journet L. (2014). VgrG, Tae, Tle, and beyond: the versatile arsenal of Type VI secretion effectors. Trends Microbiol. 22:498–507.

Durand E, Nguyen VS, Zoued A, Logger L, Péhau-Arnaudet G, Aschtgen M-SS, et al. (2015). Biogenesis and structure of a type VI secretion membrane core complex. Nature 523:555–60.

Espinosa-Urgel M, Salido A, Ramos JL. (2000). Genetic analysis of functions involved in adhesion of Pseudomonas putida to seeds. J. Bacteriol. 182:2363–9.

Filloux A. (2011). Protein Secretion Systems in Pseudomonas aeruginosa: An Essay on Diversity, Evolution, and Function. Front Microbiol 2:155.

Filloux A, Freemont P. (2016). Structural biology: Baseplates in contractile machines. Nature Microbiology 1:16104.

Finn RD, Coggill P, Eberhardt RY, Eddy SR, Mistry J, Mitchell AL, et al. (2016). The Pfam protein families database: towards a more sustainable future. Nucleic Acids Res. 44:D279–85.

Gomi M, Sonoyama M, Mitaku S. (2004). High performance system for signal peptide prediction: SOSUIsignal. Chem-Bio Info. J. 4:142–147.

580 Gotfredsen M, Gerdes K. (1998). The Escherichia coli relBE genes belong to a new toxin-
581 antitoxin gene family. Mol. Microbiol. 29:1065–76.

582 Gueguen E, Wills NM, Atkins JF, Cascales E. (2014). Transcriptional frameshifting
583 rescues Citrobacter rodentium type VI secretion by the production of two length variants
584 from the prematurely interrupted tssM gene. PLoS Genet. 10:e1004869.

585 Guzman LM, Belin D, Carson MJ, Beckwith J. (1995). Tight regulation, modulation, and
586 high-level expression by vectors containing the arabinose PBAD promoter. J. Bacteriol.
587 177:4121–30.

588 Hachani A, Allsopp L, Oduko Y, Filloux A. (2014). The VgrG proteins are 'A la carte'
589 delivery systems for bacterial type VI effectors. Journal of Biological Chemistry
590 289:jbc.M114.563429.

591 Hachani A, Lossi N, Hamilton A, Jones C, Bleves S, Albesa-Jové D, et al. (2011). Type
592 VI Secretion System in Pseudomonas aeruginosa SECRETION AND
593 MULTIMERIZATION OF VgrG PROTEINS. J Biol Chem 286:12317–12327.

594 Hachani A, Lossi NS, Filloux A. (2013). A visual assay to monitor T6SS-mediated
595 bacterial competition. J Vis Exp e50103.

596 Hachani A, Wood TE, Filloux A. (2016). Type VI secretion and anti-host effectors. Curr.
597 Opin. Microbiol. 29:81–93.

598 Haney CH, Ausubel FM. (2015). MICROBIOME. Plant microbiome blueprints. Science
599 349:788–9.

600 Haney CH, Samuel BS, Bush J, Ausubel FM. (2015). Associations with rhizosphere
601 bacteria can confer an adaptive advantage to plants. Nat Plants 1.

602 Ho B, Dong T, Mekalanos J. (2013). A View to a Kill: The Bacterial Type VI Secretion
603 System. Cell Host & Microbe 15.

604 Hoang TT, Kutchma AJ, Becher A, Schweizer HP. (2000). Integration-proficient
605 plasmids for Pseudomonas aeruginosa: site-specific integration and use for engineering
606 of reporter and expression strains. Plasmid 43:59–72.

607 Hood R, Singh P, Hsu F, Güvener T, Carl M, Trinidad R, et al. (2010). A Type VI
608 Secretion System of Pseudomonas aeruginosa Targets a Toxin to Bacteria. Cell Host
609 Microbe 7:25–37.

610 Huang H, Yuan HS. (2007). The conserved asparagine in the HNH motif serves an
611 important structural role in metal finger endonucleases. J. Mol. Biol. 368:812–21.

612 Imai K, Asakawa N, Tsuji T, Akazawa F, Ino A, Sonoyama M, et al. (2008). SOSUI-
613 GramN: high performance prediction for sub-cellular localization of proteins in gram-
614 negative bacteria. Bioinformation 2:417–21.

615 Jones C, Hachani A, Manoli E, Filloux A. (2014). An rhs gene linked to the second type
616 VI secretion cluster is a feature of the Pseudomonas aeruginosa strain PA14. J. Bacteriol.
617 196:800–10.

618 Kaniga K, Delor I, Cornelis GR. (1991). A wide-host-range suicide vector for improving
619 reverse genetics in gram-negative bacteria: inactivation of the blaA gene of Yersinia
620 enterocolitica. Gene 109:137–41.

621 Kapitein N, Bönemann G, Pietrosiuk A, Seyffer F, Hausser I, Locker JK, et al. (2013).
622 ClpV recycles VipA/VipB tubules and prevents non-productive tubule formation to
623 ensure efficient type VI protein secretion. Mol. Microbiol. 87:1013–28.

624 Katzen F, Ferreiro DU, Oddo CG, Ielmini MV, Becker A, Pühler A, et al. (1998).
625 Xanthomonas campestris pv. campestris gum mutants: effects on xanthan biosynthesis
626 and plant virulence. J. Bacteriol. 180:1607–17.

627 Kelley LA, Mezulis S, Yates CM, Wass MN, Sternberg MJ. (2015). The Phyre2 web
628 portal for protein modeling, prediction and analysis. Nat Protoc 10:845–58.

629 Krogh A, Larsson B, von Heijne G, Sonnhammer EL. (2001). Predicting transmembrane
630 protein topology with a hidden Markov model: application to complete genomes. J. Mol.
631 Biol. 305:567–80.

632 Kube S, Kapitein N, Zimniak T, Herzog F, Mogk A, Wendler P. (2014). Structure of the
633 VipA/B type VI secretion complex suggests a contraction-state-specific recycling
634 mechanism. Cell Rep 8:20–30.

635 Kube S, Wendler P. (2015). Structural comparison of contractile nanomachines. AIMS
636 Biophysics 2:88–115.

637 Kudryashev M, Wang RY, Brackmann M, Scherer S, Maier T, Baker D, et al. (2015).
638 Structure of the type VI secretion system contractile sheath. Cell 160:952–62.

639 Lebeis SL, Paredes SH, Lundberg DS, Breakfield N, Gehring J, McDonald M, et al.
640 (2015). PLANT MICROBIOME. Salicylic acid modulates colonization of the root
641 microbiome by specific bacterial taxa. Science 349:860–4.

642 Leiman PG, Basler M, Ramagopal UA, Bonanno JB, Sauder JM, Pukatzki S, et al. (2009).
643 Type VI secretion apparatus and phage tail-associated protein complexes share a common
644 evolutionary origin. Proc. Natl. Acad. Sci. U.S.A. 106:4154–9.

645 Letunic I, Doerks T, Bork P. (2015). SMART: recent updates, new developments and
646 status in 2015. Nucleic Acids Res. 43:D257–60.

647 Liang X, Moore R, Wilton M, Wong MJ, Lam L, Dong TG. (2015). Identification of
648 divergent type VI secretion effectors using a conserved chaperone domain. Proc. Natl.
649 Acad. Sci. U.S.A. 112:9106–11.

650 Lin J-SS, Ma L-SS, Lai E-MM. (2013). Systematic dissection of the agrobacterium type
651 VI secretion system reveals machinery and secreted components for subcomplex
652 formation. PloS one 8:e67647.

653 Lyons E, Freeling M. (2008). How to usefully compare homologous plant genes and
654 chromosomes as DNA sequences. Plant J. 53:661–73.

655 Ma AT, Mekalanos JJ. (2010). In vivo actin cross-linking induced by Vibrio cholerae
656 type VI secretion system is associated with intestinal inflammation. Proceedings of the
657 National Academy of Sciences of the United States of America 107:4365–70.

658 Ma L-SS, Hachani A, Lin J-SS, Filloux A, Lai E-MM. (2014). Agrobacterium
659 tumefaciens deploys a superfamily of type VI secretion DNase effectors as weapons for
660 interbacterial competition in planta. Cell Host Microbe 16:94–104.

661 Mansfield J, Genin S, Magori S, Citovsky V, Sriariyanum M, Ronald P, et al. (2012). Top
662 10 plant pathogenic bacteria in molecular plant pathology. Molecular plant pathology
663 13:614–29.

664 Marchi M, Boutin M, Gazengel K, Rispe C, Gauthier J-PP, Guillerm-Erckelboudt A-YY,
665 et al. (2013). Genomic analysis of the biocontrol strain Pseudomonas fluorescens
666 Pf29Arp with evidence of T3SS and T6SS gene expression on plant roots. Environ
667 Microbiol Rep 5:393–403.

Marshall B, Elbert A, Petren K, Rizvi S, Fink A, Ostrenga J, et al. (2015). Cystic Fibrosis Foundation Patient Registry 2014 Annual Data Report . ©2015 Cystic Fibrosis Foundation: Bethesda, Maryland, USA.

Matilla M, Ramos J, Bakker P, Doornbos R, Badri D, Vivanco J, et al. (2010). Pseudomonas putida KT2440 causes induced systemic resistance and changes in Arabidopsis root exudation. Environ Microbiol Reports 2:381–388.

Miyata ST, Kitaoka M, Brooks TM, McAuley SB, Pukatzki S. (2011). Vibrio cholerae requires the type VI secretion system virulence factor VasX to kill Dictyostelium discoideum. Infection and immunity 79:2941–9.

Molina L, Ramos C, Duque E, Ronchel MC, Garcia JM, Wyke L, et al. (2000). Survival of Pseudomonas putida KT2440 in soil and in the rhizosphere of plants under greenhouse and environmental conditions. Soil. Biol. Biochem. 32:315–321.

Moscoso JA, Mikkelsen H, Heeb S, Williams P, Filloux A. (2011). The Pseudomonas aeruginosa sensor RetS switches type III and type VI secretion via c-di-GMP signalling. Environ. Microbiol. 13:3128–38.

Mougous JD, Cuff ME, Raunser S, Shen A, Zhou M, Gifford CA, et al. (2006). A virulence locus of Pseudomonas aeruginosa encodes a protein secretion apparatus. Science 312:1526–30.

Murdoch SL, Trunk K, English G, Fritsch MJ, Pourkarimi E, Coulthurst SJ. (2011). The opportunistic pathogen Serratia marcescens utilizes type VI secretion to target bacterial competitors. J. Bacteriol. 193:6057–69.

Okonechnikov K, Golosova O, Fursov M. (2012). Unipro UGENE: a unified bioinformatics toolkit. Bioinformatics 28:1166–7.

De Pace F, Nakazato G, Pacheco A, de Paiva JB, Sperandio V, da Silveira WD. (2010). The type VI secretion system plays a role in type 1 fimbria expression and pathogenesis of an avian pathogenic Escherichia coli strain. Infect. Immun. 78:4990–8.

Petersen TN, Brunak S, von Heijne G, Nielsen H. (2011). SignalP 4.0: discriminating signal peptides from transmembrane regions. Nat. Methods 8:785–6.

Planamente S, Salih O, Manoli E, Albesa-Jové D, Freemont PS, Filloux A. (2016). TssA forms a gp6-like ring attached to the type VI secretion sheath. EMBO J.

Pukatzki S, Ma AT, Sturtevant D, Krastins B, Sarracino D, Nelson WC, et al. (2006). Identification of a conserved bacterial protein secretion system in Vibrio cholerae using the Dictyostelium host model system. Proc. Natl. Acad. Sci. U.S.A. 103:1528–33.

Ramos-Gonzalez MI, Duque E, Ramos JL. (1991). Conjugational transfer of recombinant DNA in cultures and in soils: host range of Pseudomonas putida TOL plasmids. Appl. Environ. Microbiol. 57:3020–7.

Rosales-Reyes R, Skeldon AM, Aubert DF, Valvano MA. (2012). The Type VI secretion system of Burkholderia cenocepacia affects multiple Rho family GTPases disrupting the actin cytoskeleton and the assembly of NADPH oxidase complex in macrophages. Cell. Microbiol. 14:255–73.

Russell AB, Hood RD, Bui NK, LeRoux M, Vollmer W, Mougous JD. (2011). Type VI secretion delivers bacteriolytic effectors to target cells. Nature 475:343–7.

Russell AB, Peterson SB, Mougous JD. (2014). Type VI secretion system effectors: poisons with a purpose. Nat. Rev. Microbiol. 12:137–48.

Russell AB, Wexler AG, Harding BN, Whitney JC, Bohn AJ, Goo YA, et al. (2014). A type VI secretion-related pathway in Bacteroidetes mediates interbacterial antagonism. Cell Host Microbe 16:227–36.

Salomon D, Gonzalez H, Updegraff BL, Orth K. (2013). Vibrio parahaemolyticus type VI secretion system 1 is activated in marine conditions to target bacteria, and is differentially regulated from system 2. PLoS ONE 8:e61086.

Salomon D, Kinch LN, Trudgian DC, Guo X, Klimko JA, Grishin NV, et al. (2014). Marker for type VI secretion system effectors. Proc. Natl. Acad. Sci. U.S.A. 111:9271–6.

Sambrook J, Maniatis T, Fritsch EF. (1989). Molecular Cloning: a Laboratory Manual. Cold Spring Harbor, NY: Cold Spring Harbor Laboratory.

Sana TG, Soscia C, Tonglet CMM, Garvis S, Bleves S. (2013). Divergent control of two type VI secretion systems by RpoN in Pseudomonas aeruginosa. PLoS ONE 8:e76030.

Schlieker C, Zentgraf H, Dersch P, Mogk A. (2005). ClpV, a unique Hsp100/Clp member of pathogenic proteobacteria. Biol. Chem. 386:1115–27.

727 Shneider MM, Buth SA, Ho BT, Basler M, Mekalanos JJ, Leiman PG. (2013). PAAR-
728 repeat proteins sharpen and diversify the type VI secretion system spike. Nature 500:350–
729 3.

730 Silverman JM, Agnello DM, Zheng H, Andrews BT, Li M, Catalano CE, et al. (2013).
731 Haemolysin coregulated protein is an exported receptor and chaperone of type VI
732 secretion substrates. Mol. Cell 51:584–93.

733 Silverman JM, Austin LS, Hsu F, Hicks KG, Hood RD, Mougous JD. (2011). Separate
734 inputs modulate phosphorylation-dependent and -independent type VI secretion
735 activation. Mol. Microbiol. 82:1277–90.

736 Stone M. (2016). Root and gut microbiomes are strikingly similar. Microbe 11:107–110.

737 Suarez G, Sierra JC, Sha J, Wang S, Erova TE, Fadl AA, et al. (2008). Molecular
738 characterization of a functional type VI secretion system from a clinical isolate of
739 Aeromonas hydrophila. Microb. Pathog. 44:344–61.

740 Tamura K, Stecher G, Peterson D, Filipski A, Kumar S. (2013). MEGA6: Molecular
741 Evolutionary Genetics Analysis version 6.0. Mol. Biol. Evol. 30:2725–9.

742 Unterweger D, Kostiuk B, Ötjengerdes R, Wilton A, Diaz-Satizabal L, Pukatzki S.
743 (2015). Chimeric adaptor proteins translocate diverse type VI secretion system effectors
744 in Vibrio cholerae. EMBO J. 34:2198–210.

745 Validov S, Kamilova F, Qi S, Stephan D, Wang JJ, Makarova N, et al. (2007). Selection
746 of bacteria able to control Fusarium oxysporum f. sp. radicis-lycopersici in stonewool
747 substrate. J. Appl. Microbiol. 102:461–71.

748 Vasseur P, Vallet-Gely I, Soscia C, Genin S, Filloux A. (2005). The pel genes of the
749 Pseudomonas aeruginosa PAK strain are involved at early and late stages of biofilm
750 formation. Microbiology (Reading, Engl.) 151:985–97.

751 Weinert C, Morger D, Djekic A, Grütter MG, Mittl PR. (2015). Crystal structure of
752 TRIM20 C-terminal coiled-coil/B30.2 fragment: implications for the recognition of
753 higher order oligomers. Sci Rep 5:10819.

754 Weller DM. (2007). Pseudomonas biocontrol agents of soilborne pathogens: looking back
755 over 30 years. Phytopathology 97:250–6.

Weller DM, Raaijmakers JM, Gardener BB, Thomashow LS. (2002). Microbial populations responsible for specific soil suppressiveness to plant pathogens. Annu Rev Phytopathol 40:309–48.

Wexler AG, Bao Y, Whitney JC, Bobay L-MM, Xavier JB, Schofield WB, et al. (2016). Human symbionts inject and neutralize antibacterial toxins to persist in the gut. Proceedings of the National Academy of Sciences of the United States of America 113:3639–44.

Whitney JC, Beck CM, Goo YA, Russell AB, Harding BN, De Leon JA, et al. (2014). Genetically distinct pathways guide effector export through the type VI secretion system. Mol. Microbiol. 92:529–42.

Whitney JC, Quentin D, Sawai S, LeRoux M, Harding BN, Ledvina HE, et al. (2015). An Interbacterial NAD(P)(+) Glycohydrolase Toxin Requires Elongation Factor Tu for Delivery to Target Cells. Cell.

Winsor GL, Griffiths EJ, Lo R, Dhillon BK, Shay JA, Brinkman FS. (2016). Enhanced annotations and features for comparing thousands of Pseudomonas genomes in the Pseudomonas genome database. Nucleic Acids Res. 44:D646–53.

Yu NY, Wagner JR, Laird MR, Melli G, Rey S, Lo R, et al. (2010). PSORTb 3.0: improved protein subcellular localization prediction with refined localization subcategories and predictive capabilities for all prokaryotes. Bioinformatics 26:1608–15.

Zheng J, Ho B, Mekalanos JJ. (2011). Genetic analysis of anti-amoebae and anti-bacterial activities of the type VI secretion system in Vibrio cholerae. PLoS ONE 6:e23876.

Zoued A, Brunet YR, Durand E, Aschtgen M-SS, Logger L, Douzi B, et al. (2014). Architecture and assembly of the Type VI secretion system. Biochim. Biophys. Acta 1843:1664–73.

Figures legends

Figure 1. T6SS clusters in *P. putida* KT2440. (**a**) Schematic representation of the T6SS structure. (**b**) Distribution of the K1-, K2- and K3-T6SS clusters (blue), and the *vgrG* (yellow) and *hcp* (purple) genes in the KT2440 genome. (**c-e**) Genomic organisation of the *P. putida* T6SSs cluster, including K1 (**c**), K2 and K3 (**d**) or the *vgrG* and *hcp* orphan clusters (**e**). The colour code of the genes correlates with the colour code shown in panel **a**. The asterisk (*) in the *tssC2*, *vgrG2* and *hcp4* genes indicates that these genes contain premature stop codons.

Figure 2. Phylogenetic distribution of T6SS clusters in *P. putida* species. Maximum-likelihood tree with 1000 bootstrap replicates were built with Mega 6 for the core component protein TssB. T6SS cluster nomenclature (Boyer et al., 2009, Barret et al., 2011) is used to show the major phylogenetic clusters. Three main groups are clearly distinguishable: group 1.2 (green), group 2 (red) and group 4B (blue). *P. aeruginosa* and *A. tumefaciens* T6SSs loci are included into the phylogenetic tree to illustrate all the subgroups: 1.1 (*P. aeruginosa* H2), 1.2 (*P. putida* K2-K3), 2 (*P. putida* W619), 3 (*P. aeruginosa* H1), 4A (*P. aeruginosa* H3), 4B (*P. putida* K1) and 5 (*A. tumefacines*).

Figure 3. Functionality of the *P. putida* K1-T6SS. (**a**) Production and secretion of Hcp1 in the *P. putida* KT2440 wild-type and the Δ*tssA1* mutant strains. The HA tagged Hcp1 protein was detected by western-blot analysis using an anti-HA antibody. Detection of the β subunit of the RNA polymerase (β-RNAP) was used as control. The position of the molecular size marker (in kDa) is indicated. (**b**) Competition assay between *P. putida* and a *lacZ*-encoding *E. coli* strain. Blue patches on X-gal-containing LB plates indicate *E. coli* survival. The top row shows the growth of *E. coli*, *P. putida* KT2440 wild-type strain

and a battery of *P. putida* mutants in K1-T6SS genes. The bottom row shows the growth of mixed *E. coli*/*P. putida* cultures after 5h of co-incubation.

Figure 4. *P. putida* KT2440 T6SS effectors. (**a**) The domain organization of the putative effectors is shown, with PAAR motifs indicated in orange, MIX-motifs in blue, Rhs domains in green, HNH nuclease motifs (Tox-HNH and Tox-SHH) in purple, colicin motifs in yellow, and the Tox-61 domain in pink. Multiple sequence alignments of the PAAR (**b**) and MIX (**c**) protein motifs are represented. The KT2440 T6SS effectors identified in this work are indicated in blue. The sequence of known T6SS effectors containing these motifs was retrieved from the NCBI database (http://www.ncbi.nlm.nih.gov/Structure/cdd/cdd.shtml). Conservation logos of the motifs are indicated above the alignment. Conserved residues are highlighted according to the amino acid characteristic: hydrophobic (black), small (pink), positive (blue), negative (yellow) and polar (purple, light blue, red).

Figure 5. *P. putida* KT2440 T6SS nucleases. **(a-b)** Multiple sequence alignments of the C-terminal domains of Tke2 **(a)** and Tke4 **(b)** effectors (blue) with known proteins of the family (black). Conservation logos of the motifs HNH **(a)** and SHH **(b)** are indicated above the alignment. Conserved residues are indicated with the colour code used in figure 4. A representation of the structural model of the C-terminal domain of the Tke2 effector (magenta) superimposed on the colicin E7 structure (blue; PDB: 2JB0) is shown on the right of panel a. Side chains of the active site residues are shown. **(c)** Multiple sequence alignment of T6SS colicin effectors (blue) with known proteins of the family (black). The secondary structure prediction (ssp) for effector Tke7 is shown above the alignment. A

structural alignment of the Tke7 effector model (magenta) with the colicin S4 (blue, PDB: 3FEW) is shown on the right.

Figure 6. Toxicity and secretion of the Tke2 effector. (**a**) The growth of *E. coli* K12 cells harbouring the pTke2-CT and pTki2 plasmids containing the C-terminal toxin domain of the *tke2* effector and the *tki2* immunity genes, respectively, was determined by measuring the OD at 600 nm. At time zero either 1 mM IPTG and/or 0.02% (w/v) arabinose were added to the LB medium to induce expression of the *tke2-CT* or/and *tki2* genes, respectively. (**b**) Western blot analyses using an anti-V5 or anti-HA monoclonal antibody to detect the Tke2-CT-V5 or Tki2-HA tagged proteins. Proteins were prepared from *E. coli* K12 cells grown during 10 hours in presence (+) or absence (-) of 1 mM IPTG and/or 0.02% (w/v) arabinose. (**c**) The indicated *P. putida* KT2440 strains bearing a *tke2*-V5 tagged gene were grown in TSB medium for 5 hours. Tke2-V5 was detected in the whole cell and supernatant fractions using a monoclonal anti-V5 antibody. Detection of the β subunit of the RNA polymerase (β-RNAP) was used as control. The position of the molecular size marker (in kDa) is indicated.

Figure 7. Bactericidal activity of *P. putida* KT2440 against a panel of phytopathogens. *X. campestris*, *A. tumefaciens*, *P. carotovorum* and *P. syringae pv. tomato* strains harbour the pRL662-gfp plasmid that confers gentamycin resistance. The *P. putida* KT2440 wild-type (WT) and its isogenic Δ*tssA1*Δ*tssM2*Δ*tssM3* triple mutant (ΔT6SS) were co-incubated with the phytopathogens for 24 hours. CFU quantifications were performed upon gentamycin selection. The average ± SD from at least three biological replicates is plotted.

Figure 8. *In planta* competition assay between the biocontrol strain *P. putida* KT2440 and the phytopathogen *X. campestris*. (**a**) Leaves of *Nicotiana benthamiana* 24 hours after being infiltrated with *X. campestris* (pRL662-gfp) (expressing a plasmid-encoded green fluorescence protein), the *P. putida* KT2440 wild-type (WT), or its isogenic Δ*tssA1*Δ*tssM2*Δ*tssM3* triple mutant (ΔT6SS). (**b**) Leaves of *Nicotiana benthamiana* 5 days after co-infiltration of *X. campestris* (pRL662-gfp) with the indicated *P. putida* strain. In (**a**) and (**b**) the leaves were also visualized by fluorescence microscopy using a Leica M205FA stereomicroscope. The necrotic areas resulting from *X. campestris* infection are marked. The deep brown zone of necrosis is spread on a large portion of the leave (right panel) while such spread is far more restricted when the phytopathogen is co-inoculated with a T6SS positive *P. putida* strain (left panel) (**c**) Quantification of *X. campestris* (pRL662-gfp) CFU recovered from *Nicotiana benthamiana* leaves after 24-hour of co-infiltration with the indicated *P. putida* strain. *X. campestris* CFU were quantified after Gm selection. Graphs represent mean +SD, of at least 5 biological replicates with two technical replicates per experiment, statistical significance is indicated t-test $P < 0.001$.

Figure 1

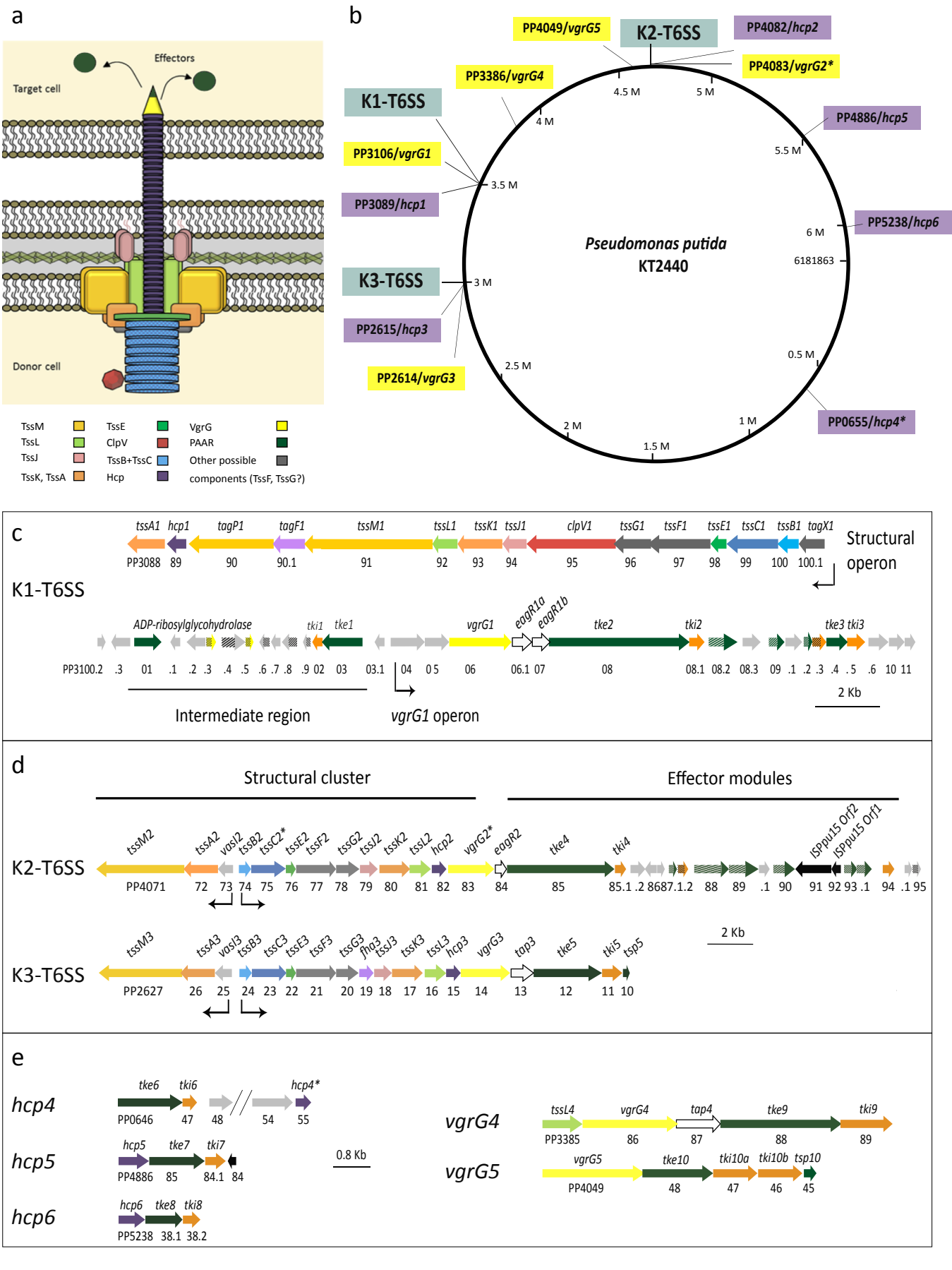
a
Effectors
Target cell
Donor cell
TssM
TssL
TssJ
TssK, TssA
TssE
ClpV
TssB+TssC
Hcp
VgrG
PAAR
Other possible components (TssF, TssG?)
b
PP4049/vgrG5
K2-T6SS
PP4082/hcp2
PP4083/vgrG2*
PP3386/vgrG4
K1-T6SS
PP4886/hcp5
PP3106/vgrG1
PP3089/hcp1
PP5238/hcp6
Pseudomonas putida
KT2440
6181863
K3-T6SS
PP2615/hcp3
PP2614/vgrG3
PP0655/hcp4*
4.5 M
5 M
4 M
5.5 M
3.5 M
6 M
3 M
0.5 M
2.5 M
1 M
2 M
1.5 M
c
K1-T6SS
tssA1 hcp1 tagP1 tagF1 tssM1 tssL1 tssK1 tssJ1 clpV1 tssG1 tssF1 tssE1 tssC1 tssB1 tagX1
PP3088 89 90 90.1 91 92 93 94 95 96 97 98 99 100 100.1
Structural operon
ADP-ribosylglycohydrolase tki1 tke1 vgrG1 eagR1a eagR1b tke2 tki2 tke3 tki3
PP3100.2 .3 01 .1 .2 .3 .4 .5 .6 .7 .8 .9 02 03 03.1 04 05 06 06.1 07 08 08.1 08.2 08.3 09 .1 .2 .3 .4 .5 .6 10 11
2 Kb
Intermediate region
vgrG1 operon
d
Structural cluster
Effector modules
K2-T6SS
tssM2 tssA2 vasI2 tssB2 tssC2* tssE2 tssF2 tssG2 tssJ2 tssK2 tssL2 hcp2 vgrG2* eagR2 tke4 tki4 ISPpu15 Orf2 ISPpu15 Orf1
PP4071 72 73 74 75 76 77 78 79 80 81 82 83 84 85 85.1 .2 86 87.1.2 88 89 .1 90 91 92 93 .1 94 .1 95
2 Kb
K3-T6SS
tssM3 tssA3 vasI3 tssB3 tssC3 tssE3 tssF3 tssG3 fha3 tssJ3 tssK3 tssL3 hcp3 vgrG3 tap3 tke5 tki5 tsp5
PP2627 26 25 24 23 22 21 20 19 18 17 16 15 14 13 12 11 10
e
hcp4
tke6 tki6 hcp4*
PP0646 47 48 54 55
hcp5
hcp5 tke7 tki7
PP4886 85 84.1 84
0.8 Kb
hcp6
hcp6 tke8 tki8
PP5238 38.1 38.2
vgrG4
tssL4 vgrG4 tap4 tke9 tki9
PP3385 86 87 88 89
vgrG5
vgrG5 tke10 tki10a tki10b tsp10
PP4049 48 47 46 45

Figure 2

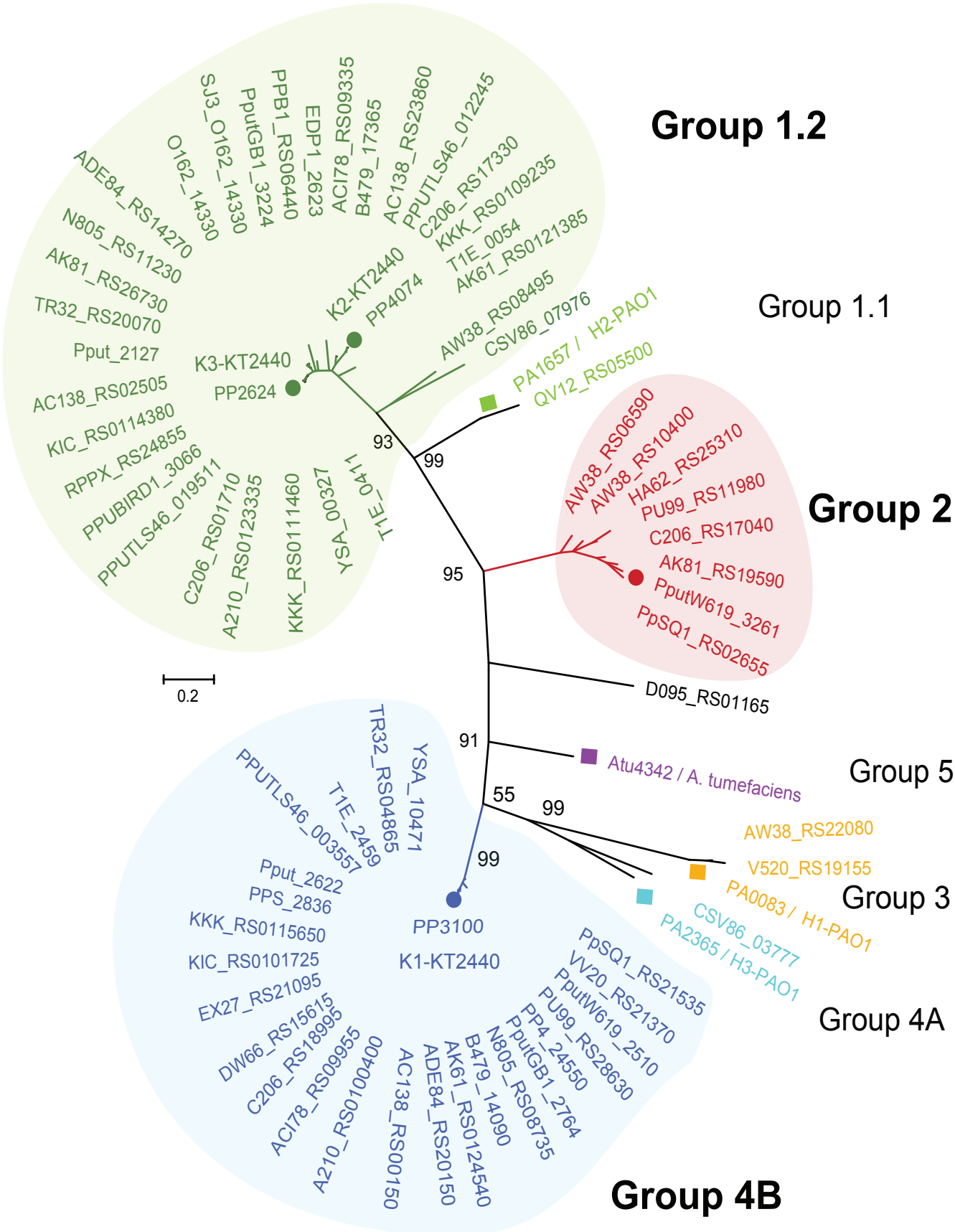
Group 1.2
Group 1.1
Group 2
Group 5
Group 3
Group 4A
Group 4B
ADE84_RS14270
N805_RS11230
AK81_RS26730
TR32_RS20070
Pput_2127
AC138_RS02505
KIC_RS0114380
RPPX_RS24855
PPUBIRD1_3066
PPUTLS46_019511
O162_14330
SJ3_O162_14330
PputGB1_3224
PPB1_RS06440
EDP1_2623
ACI78_RS09335
B479_17365
AC138_RS23860
PPUTLS46_012245
C206_RS17330
KKK_RS0109235
T1E_0054
AK61_RS0121385
AW38_RS08495
CSV86_07976
K2-KT2440
PP4074
K3-KT2440
PP2624
PA1657 / H2-PAO1
QV12_RS05500
C206_RS01710
A210_RS0123335
KKK_RS0111460
YSA_00327
T1E_1040
93
99
95
AW38_RS06590
AW38_RS10400
HA62_RS25310
PU99_RS11980
C206_RS17040
AK81_RS19590
PputW619_3261
PpSQ1_RS02655
D095_RS01165
0.2
91
Atu4342 / A. tumefaciens
55
99
AW38_RS22080
V520_RS19155
PA0083 / H1-PAO1
CSV86_03777
PA2365 / H3-PAO1
99
PPUTLS46_003557
T1E_2459
TR32_RS04865
YSA_10471
Pput_2622
PPS_2836
KKK_RS0115650
KIC_RS0101725
EX27_RS21095
DW66_RS15615
C206_RS18995
ACI78_RS09955
A210_RS0100400
PP3100
K1-KT2440
AC138_RS00150
ADE84_RS20150
AK61_RS0124540
B479_14090
N805_RS08735
PputGB1_2764
PP4_24550
PU99_RS28630
PputW619_2510
VV20_RS21370
PpSQ1_RS21535

Figure 3

a

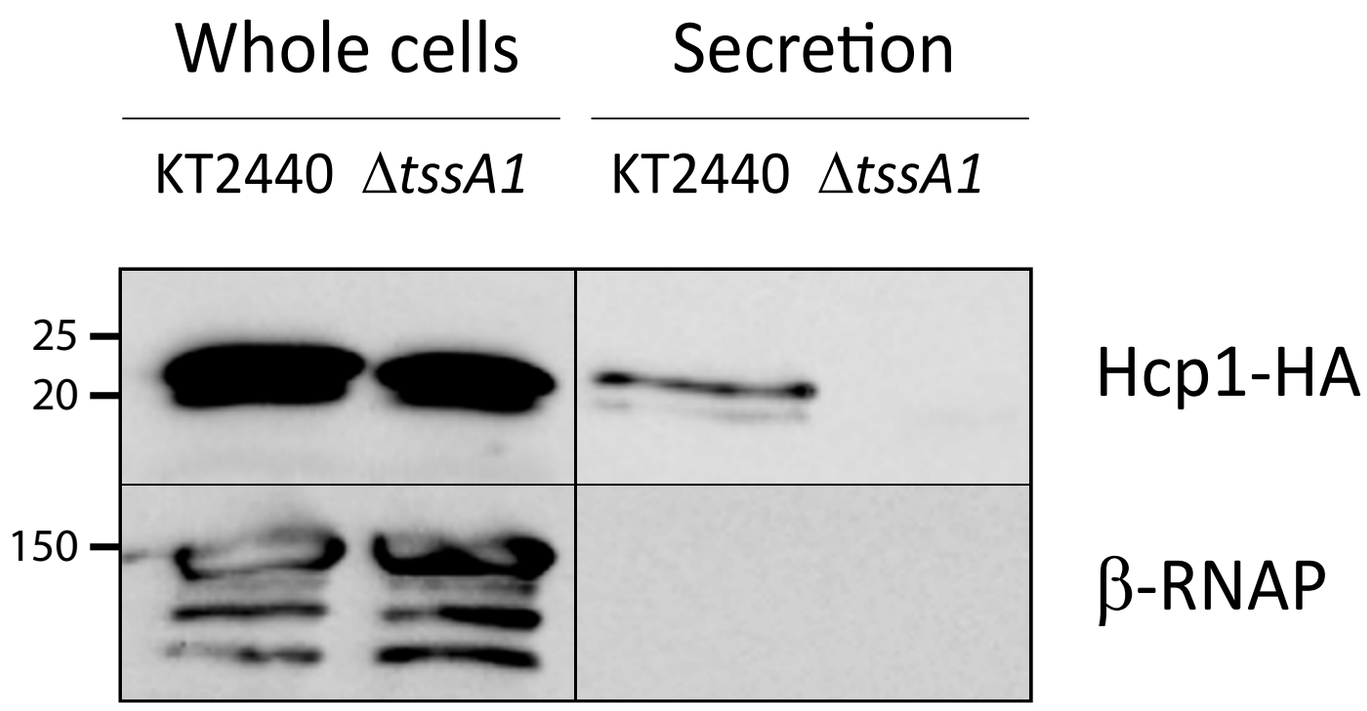
Whole cells
Secretion
KT2440
ΔtssA1
KT2440
ΔtssA1
25
20
150
Hcp1-HA
β-RNAP

b

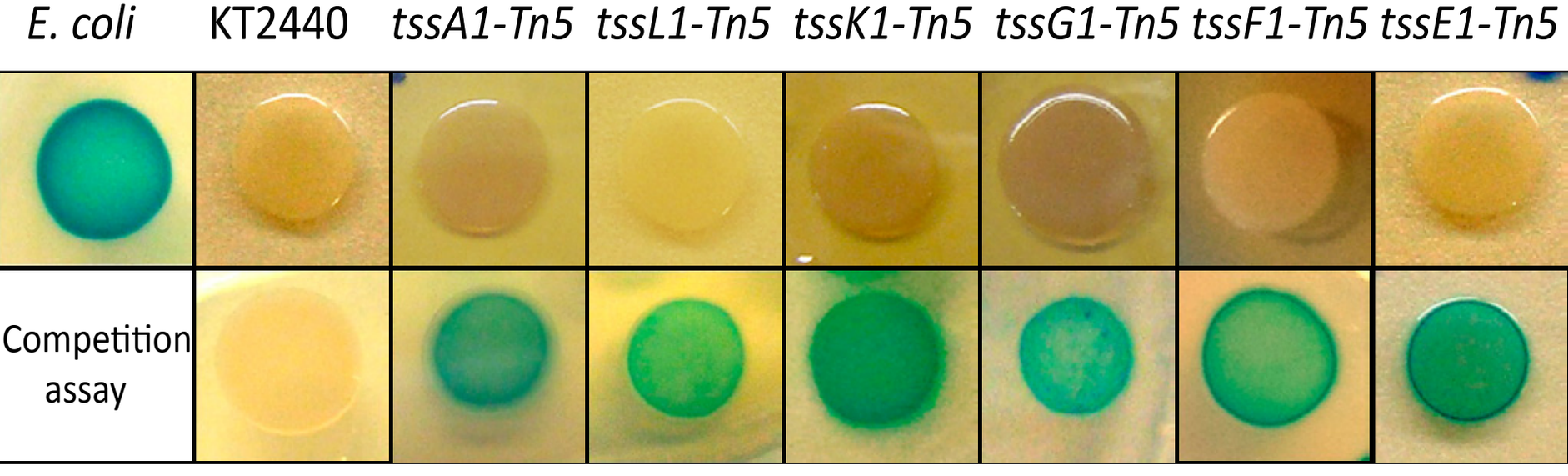
E. coli
KT2440
tssA1-Tn5
tssL1-Tn5
tssK1-Tn5
tssG1-Tn5
tssF1-Tn5
tssE1-Tn5
Competition assay

Figure 4

a

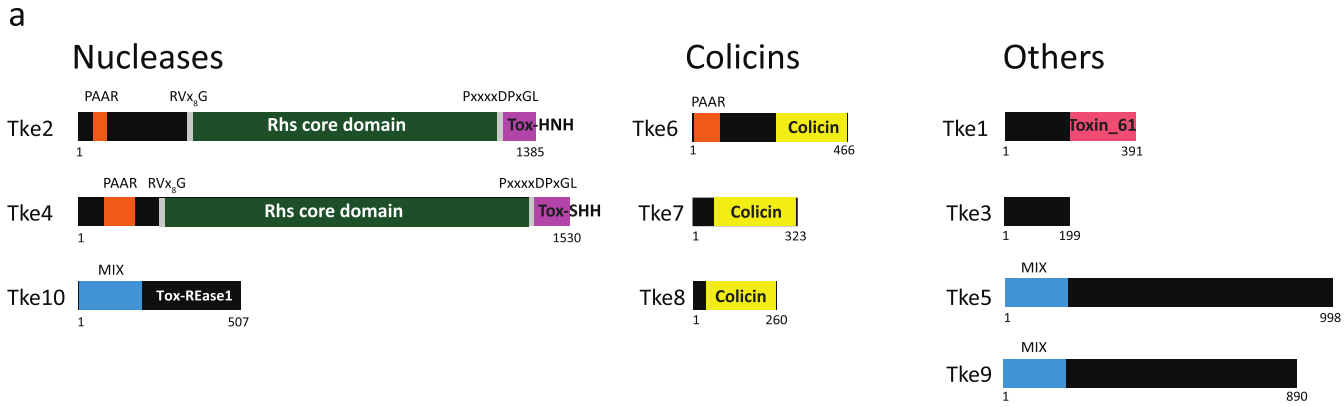
Nucleases
Colicins
Others
PAAR
RVx8G
PxxxxDPxGL
Tke2
Rhs core domain
Tox-HNH
1
1385
Tke4
Tox-SHH
1530
MIX
Tke10
Tox-REase1
507
Tke6
Colicin
466
Tke7
323
Tke8
260
Tke1
Toxin_61
391
Tke3
199
Tke5
998
Tke9
890

b

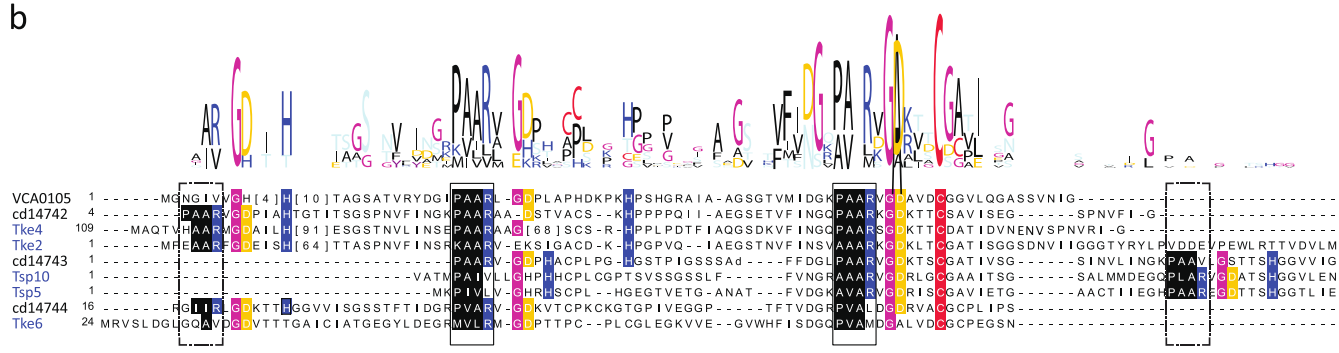
VCA0105
cd14742
Tke4
Tke2
cd14743
Tsp10
Tsp5
cd14744
Tke6

c

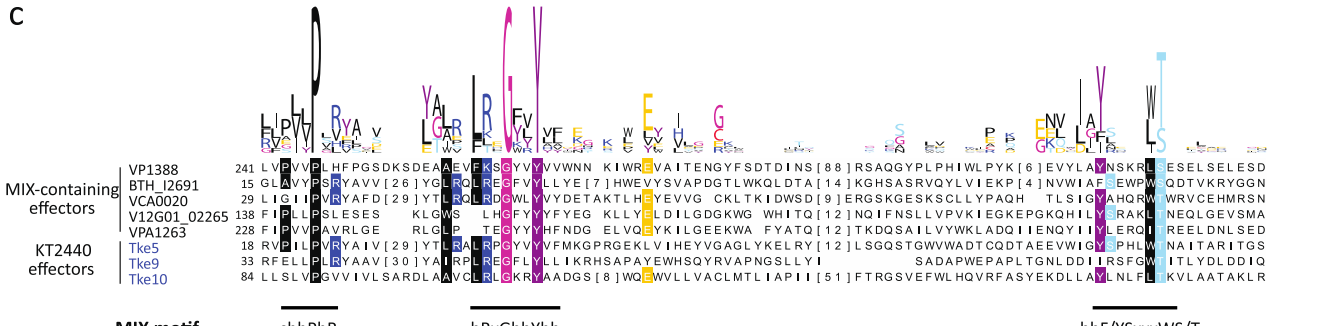
MIX-containing effectors
VP1388
BTH_I2691
VCA0020
V12G01_02265
VPA1263
KT2440 effectors
Tke5
Tke9
Tke10
MIX motif
shhPhR
hRxGhhYhh
hhF/YSxxxWS/T

Figure 5

a

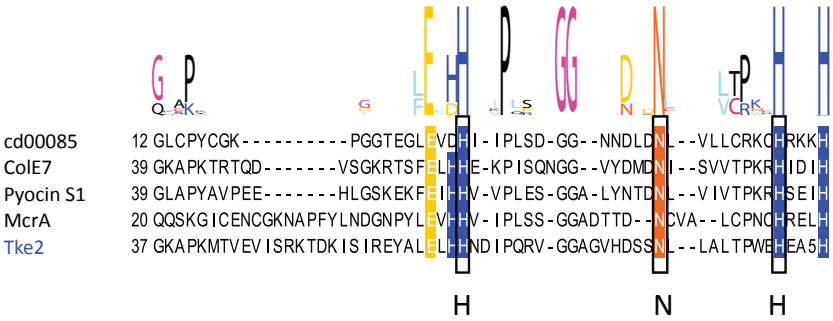
cd00085 12 GLCPYCGK----------PGGTEGLEVDHI-IPLSD-GG--NNDLDNL--VLLCRKCHRKKH
ColE7 39 GKAPKTRTQD-------VSGKRTSFELHHE-KPISQNGG--VYDMDNI--SVVTPKRHIDIH
Pyocin S1 39 GLAPYAVPEE-------HLGSKEKFEIHHV-VPLES-GGA-LYNTDNL--VIVTPKRHSEIH
McrA 20 QQSKGICENCGKNAPFYLNDGNPYLEVHHV-IPLSS-GGADTTD--NCVA--LCPNCHRELH
Tke2 37 GKAPKMTVEVISRKTDKISIREYALELHHNDIPQRV-GGAGVHDSSNL--LALTPWEHEA5H
H
N
H

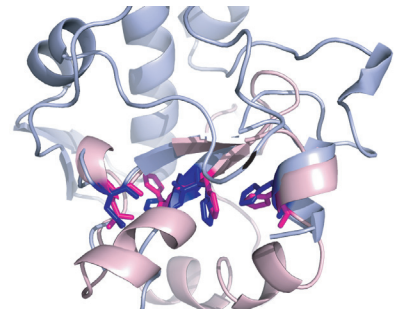

b


pfam15652 1 SDSPLQSHHGIQDEWAKKNVPGYGYRLAPAILLLS4PHAIISAAQRAQRDRRTAEGVGKWNT
PSPPH_5072 40 KNLGLDSHHVGQKDLMKDLVEGYDPATAPAMLVPRVGHTVSKEGVGIVSRSRINPNTGLPFT
Aave_3481 4 RPSDTESHHIIQDAWAKSQIGKQ3TYGAPAILLQNGPHDIANAAQNARRDARLATGRGKWES
Bcen3344 1 SNSPLENHHGVLDVWMAKNVPDY4PIKSPTIALSAESHAATKAAYRDWLTMKTGRPVGGKVD
Tke4 16 SNSPLENHHGILDIWAAQNVPSYGG3KGSPTIVLS2NHAATKAVYREWLREKTGKPVGGKVD
SHH

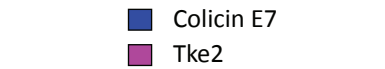
Colicin E7
Tke2

c


Pα1 Pα2 Pα3
Tke7 ssp HCCCCCHHHHHHHHHHHHHHHHHCCCCCEEHHHHHHHHHHHHHHHHHHHHHHHHHHH---CCCCCCCHHHHHHHHHHHHHH
Colicin S4 23 SMNRDRIQ SDVLNKAA EVISDIGNKVGDYLGDAYKSLAREIADDVKNFQGKTIRSY
Tke7 79 ELNGGGFDGFLLENFELLQSLLARASIGAGTASDAWSKHLEAIKKTLEEIEQLHRDYLL KGTLKARDEFYSKRTALFLKLE
Colicin N 15 KEEKEKNE KEALLKAS ELVSGMGDKLGEYLGVKYKNVAKEVANDIKNFHGRNIRSY
Tke6 14 AVLDFAESDFMMEYQAEIAGLLSDASLSMGVGKDMMDHGLRQLRSTLGNIERLHQQEFL RHGHLNSPSFFAERRLLLEQLD
Tke8 14 EVNGAGVDDFLLDNYEMLNSFLAHASMGAGAVSDGWSRHLDAIKETLGQIEQLHRDYLG GGTIKARDEFYAKRMVLFIRLE
Pα4 Pα5 Pα6
Tke7 ssp HHHHHHHHHHCCCCHHHHHHHHCCCHHHHCCCCHHHHHHHHHHHHHHHHHHHCCEEEEEEECCCHHHHHHHHCCCCHHHC
Colicin S4 79 DDAMASLNKVLSNPGFKFNRADS DALANVWRSIDAQDMANKLGNISKAF KFADVVMKVEKVREKSIEGYETG
Tke7 160 EAQLDSMATYGVGLRNGGKIKHALDISTKRFLHGGEIKGYAEKISGVAKAANWIKKGTYLGMALDVASTELSIRNACVLGREEE
Colicin N 71 NEAMASLNKVLANPKMKVNKSDK DAIVNAWKQVNAKDMANKIGNLGKAF KVADLAIKVEKIREKSIEGYNTG
Tke6 95 GQLKATFLNKHLNLGAYERLKKSLNISTKSLVHHWSKAGGPGQIPGYATYLDKVAKLSKYLRYGGHVGIGLGGTSSYLKVQEAC
Tke8 95 EQLDRLAAYGSGLRKKGKAKRTLGISTKSYLHAGEIVGYAEKIAGVSKAANLIKNGTYIGIGLDVAATGLSIHQACTLGREDEC
Pα7 Pα8 Pα9 Pα10
Tke7 ssp CEEEEEEEHHHHHHHHHHHHHHHHHHHHHHHHHHHHHCCCCHHHHHHHHHHHHHHHHHHHHHHHHHHHH
Colicin S4 151 NWGPLMLEVESWVLSGIASAVALGVFSATLGAYALSLGAPAIAVGIVGI LLAAVVGALLDDKFADALNKEI
Tke7 244 CRKAEYVERTSLVASLGLGGMGGHVGGLLGPIACVAVGIPTGGTATFACAVLGGAAGGIAGGEFGEVLGESV
Colicin N 143 NWGPLLLEVESWIGGVVAGVAISLFGAVLSFLPIS GLAVTALGVIGIM TISYLSSFIDANRVSNINNII
Tke6 179 RAGETEGCKKIRLSEAGAFAGGLAGGIVGGKIAGITALAVCGVFSAGTAGFGAPVCGIALVGGGAFAGSIAG
Tke8 179 AQARYVEGGALIGSIGGSIAGGAVGGAIATVVCTAVLGIPTGGSGALACAVLGGTLGGKIGGDKGGQGGEYF

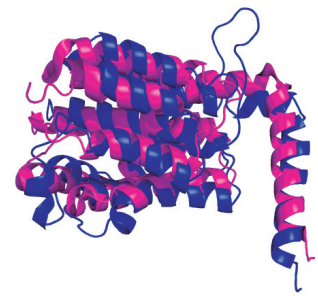

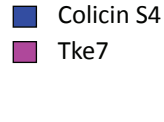
Colicin S4
Tke7

Figure 6

a

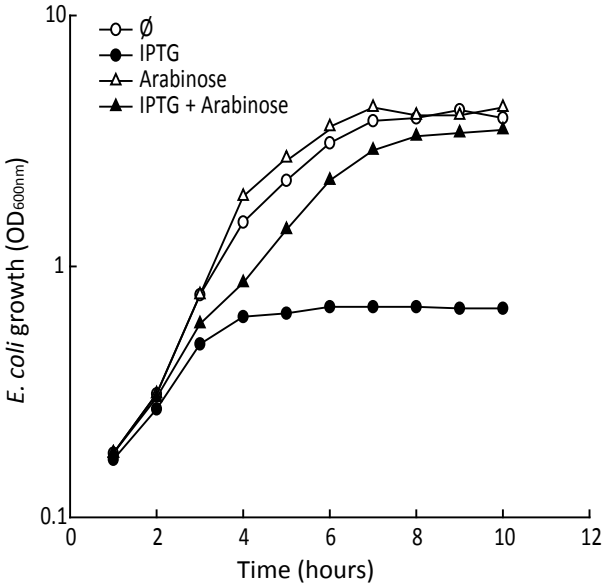
Ø
IPTG
Arabinose
IPTG + Arabinose
10
1
0.1
E. coli growth (OD600nm)
0
2
4
6
8
10
12
Time (hours)

b

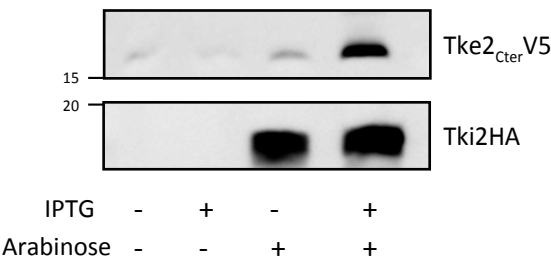
Tke2CterV5
Tki2HA
15
20
IPTG - + - +
Arabinose - - + +

c

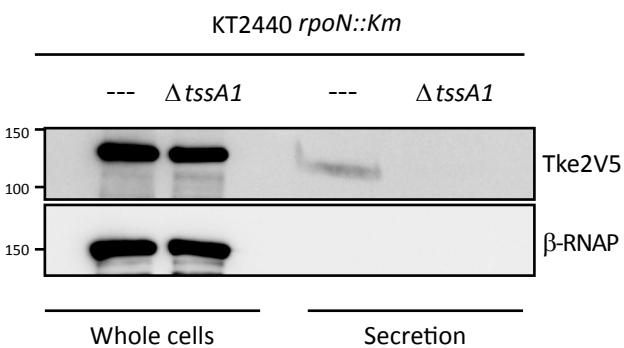
KT2440 rpoN::Km
--- ΔtssA1 --- ΔtssA1
150
100
150
Tke2V5
β-RNAP
Whole cells
Secretion

Figure 7

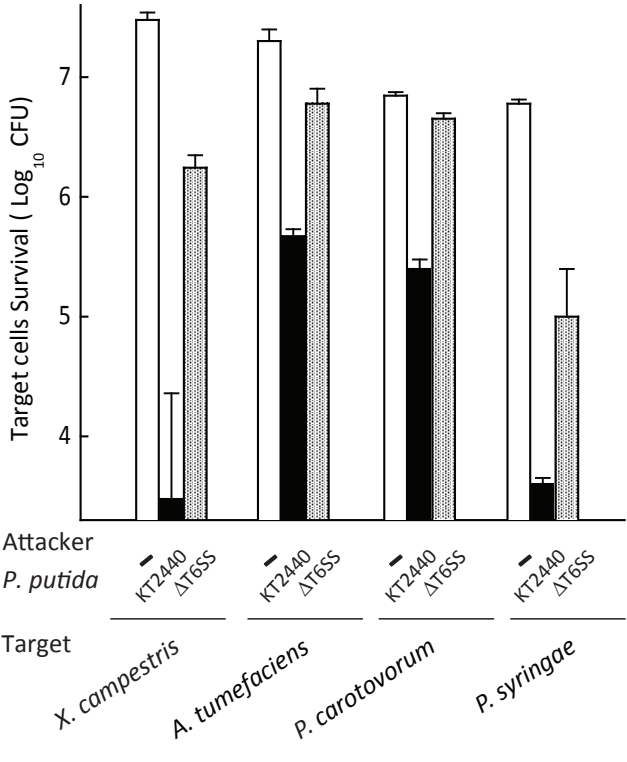
Target cells Survival (Log10 CFU)
7
6
5
4
Attacker
P. putida
–
KT2440
ΔT6SS
Target
X. campestris
A. tumefaciens
P. carotovorum
P. syringae

Figure 8

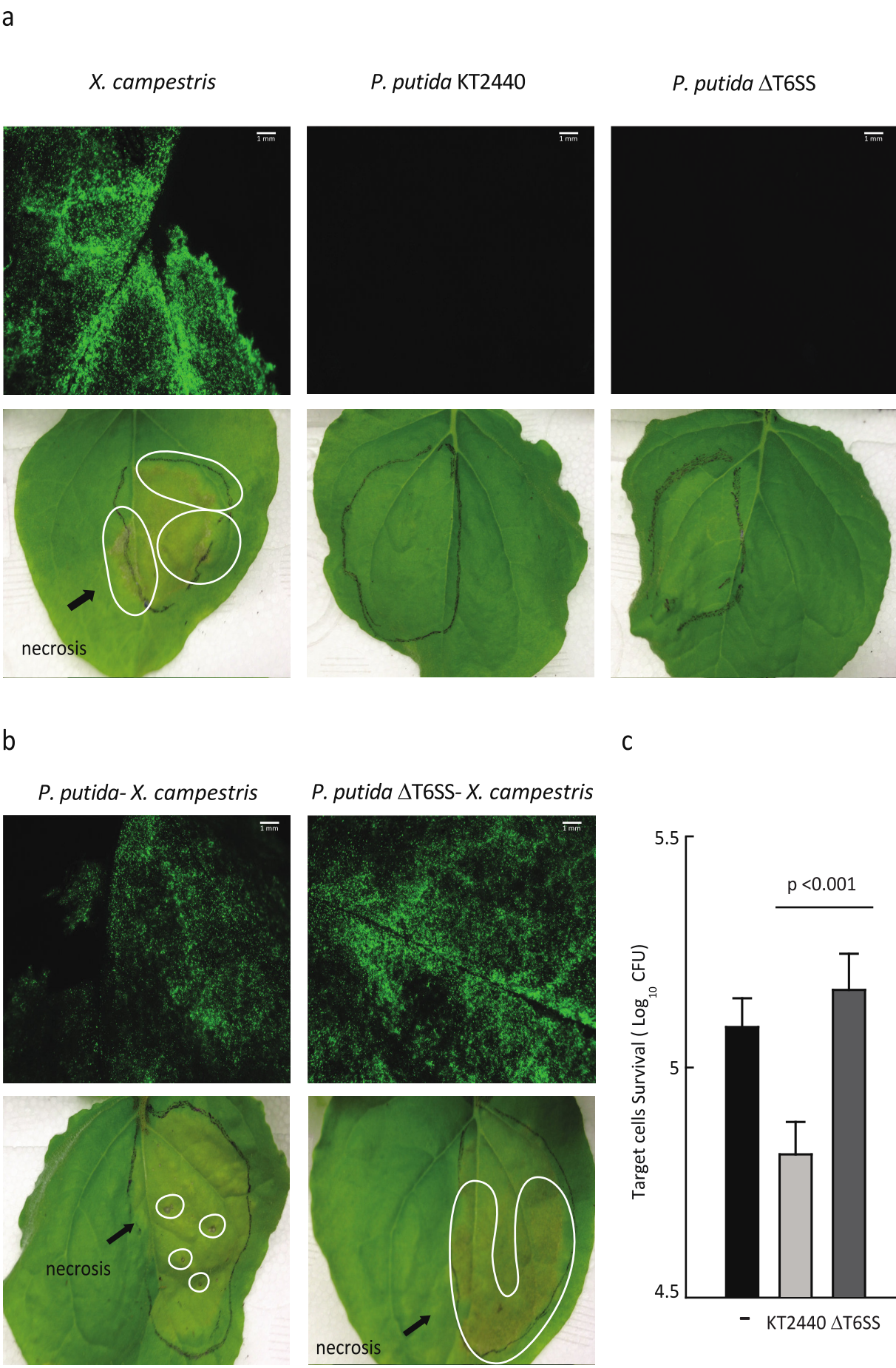
a
X. campestris
P. putida KT2440
P. putida ΔT6SS
1 mm
necrosis
b
P. putida- X. campestris
P. putida ΔT6SS- X. campestris
1 mm
necrosis
necrosis
c
5.5
5
4.5
p <0.001
Target cells Survival (Log10 CFU)
-
KT2440
ΔT6SS

Figure S1

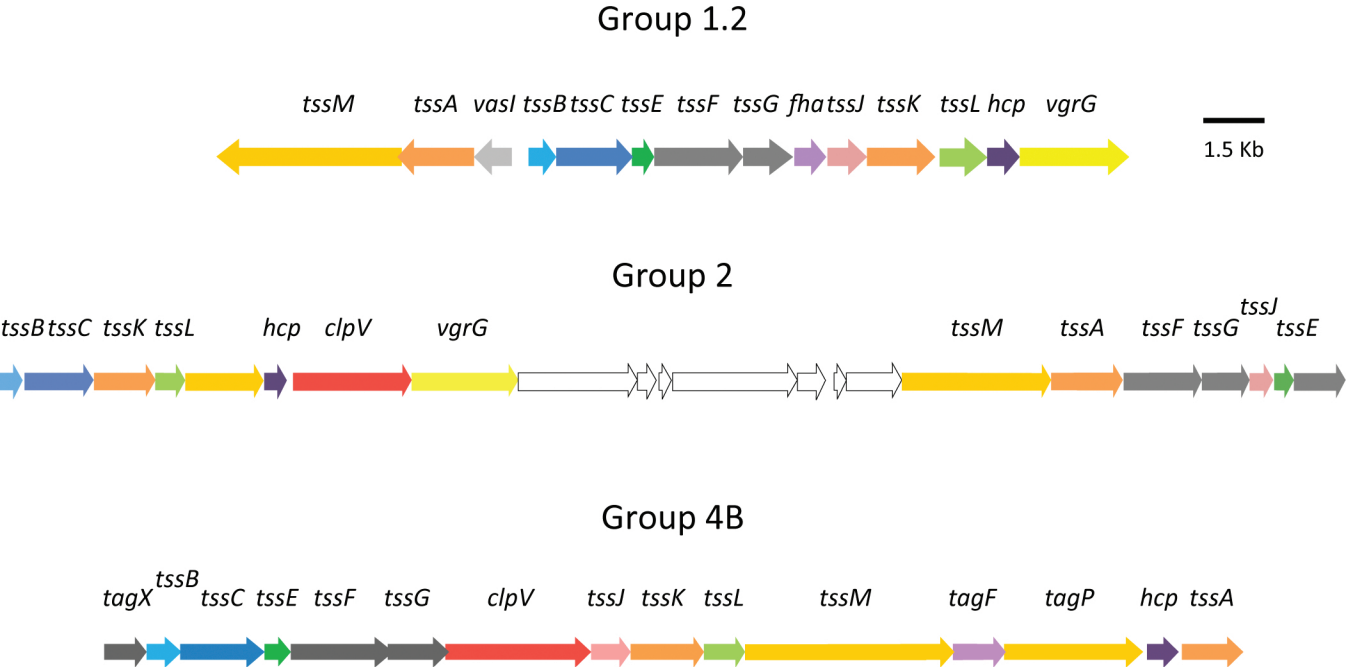
Group 1.2
tssM
tssA
vasI
tssB
tssC
tssE
tssF
tssG
fha
tssJ
tssK
tssL
hcp
vgrG
1.5 Kb
Group 2
tssB
tssC
tssK
tssL
hcp
clpV
vgrG
tssM
tssA
tssF
tssG
tssJ
tssE
Group 4B
tagX
tssB
tssC
tssE
tssF
tssG
clpV
tssJ
tssK
tssL
tssM
tagF
tagP
hcp
tssA

Figure S2

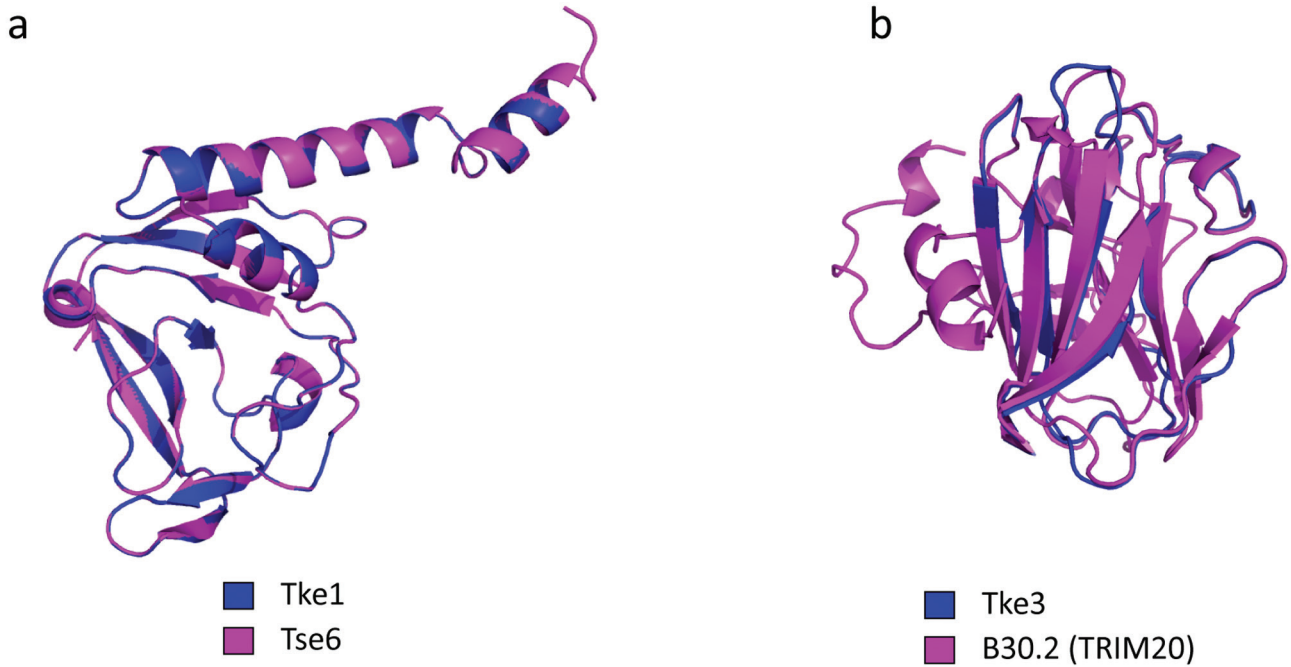

Figure S3

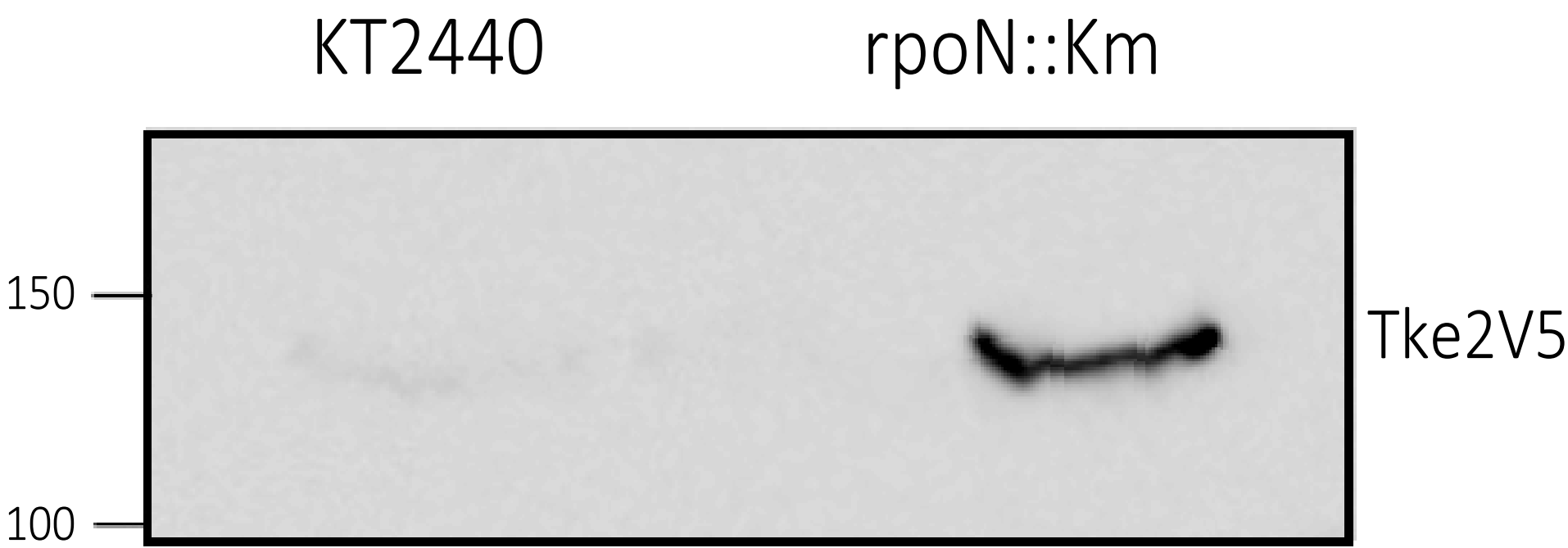

Figure S4

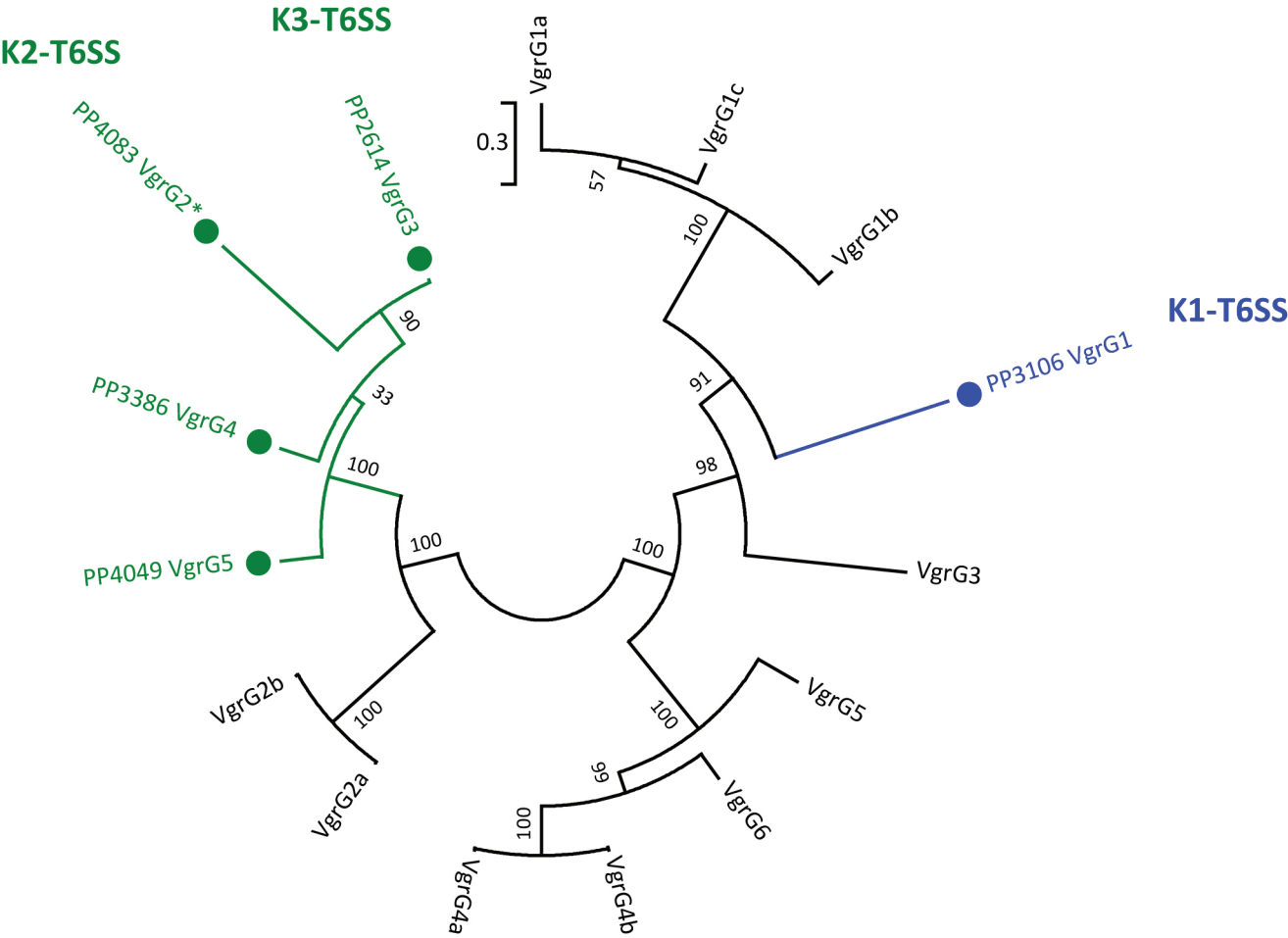
K2-T6SS
K3-T6SS
K1-T6SS
PP4083 VgrG2*
PP2614 VgrG3
PP3386 VgrG4
PP4049 VgrG5
PP3106 VgrG1
VgrG1a
VgrG1c
VgrG1b
VgrG3
VgrG5
VgrG6
VgrG4b
VgrG4a
VgrG2b
VgrG2a
0.3
57
100
91
98
100
100
100
100
90
33
100
100
100
99
100

Figure S5

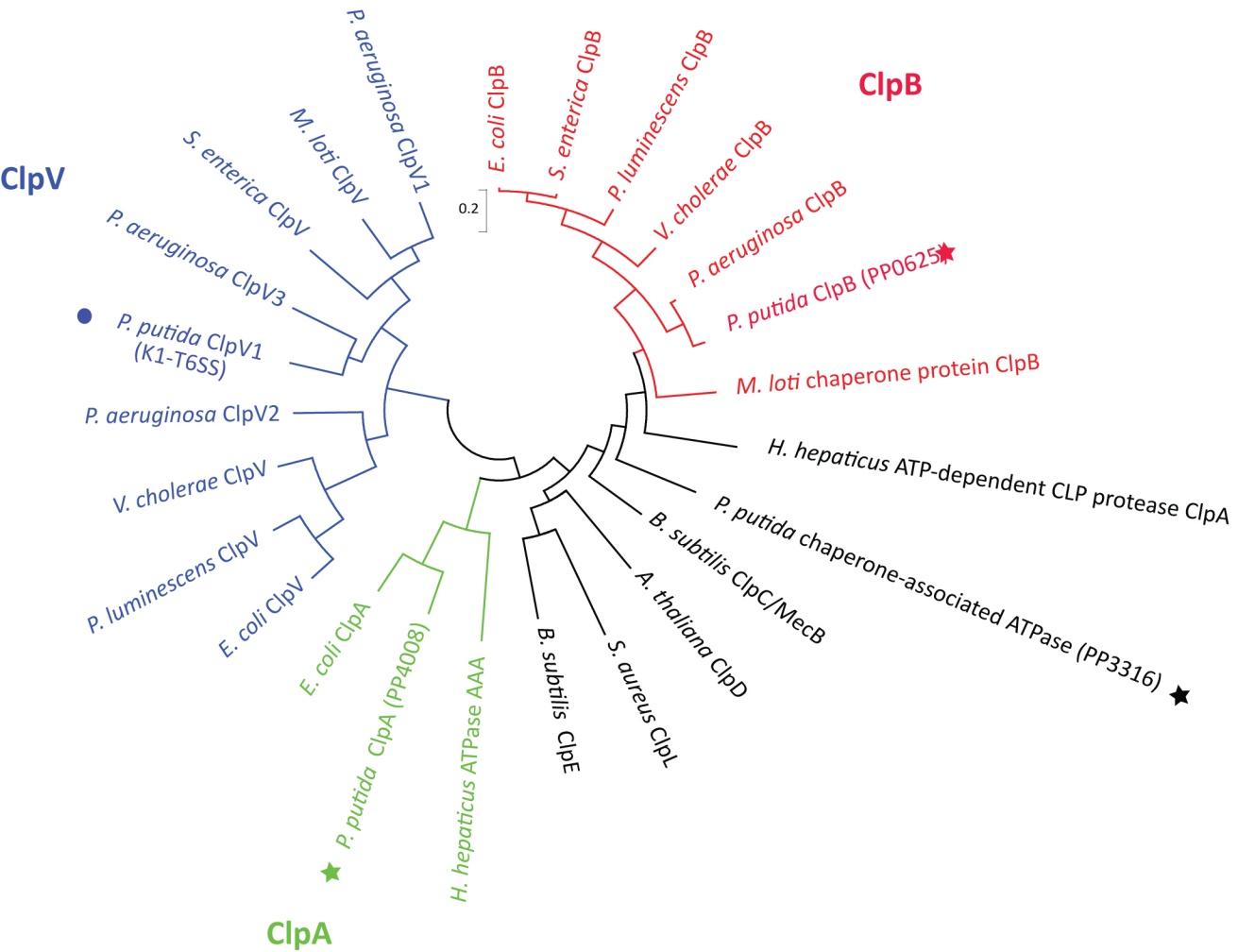
ClpV
ClpB
ClpA
0.2
P. aeruginosa ClpV1
M. loti ClpV
S. enterica ClpV
P. aeruginosa ClpV3
P. putida ClpV1 (K1-T6SS)
P. aeruginosa ClpV2
V. cholerae ClpV
P. luminescens ClpV
E. coli ClpV
E. coli ClpB
S. enterica ClpB
P. luminescens ClpB
V. cholerae ClpB
P. aeruginosa ClpB
P. putida ClpB (PP0625)
M. loti chaperone protein ClpB
H. hepaticus ATP-dependent CLP protease ClpA
P. putida chaperone-associated ATPase (PP3316)
B. subtilis ClpC/MecB
A. thaliana ClpD
S. aureus ClpL
B. subtilis ClpE
H. hepaticus ATPase AAA
P. putida ClpA (PP4008)
E. coli ClpA

Figure S6

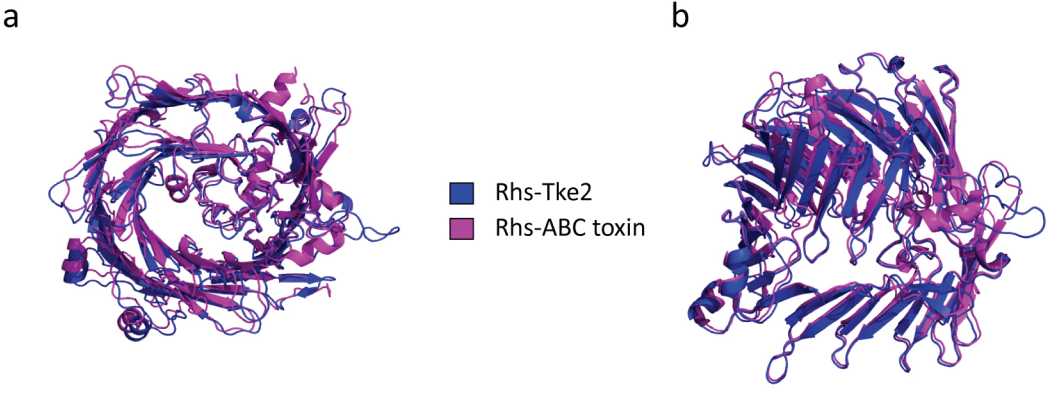

Table S1: Bacterial strains and plasmids used in this work

Bacterial strain	Description[a]	Source or reference
E. coli		
DH5α	*supE44*Δ*lacU169* (φ80 *lacZ*ΔM15) *hsdR1 recA1 endA1 gyrA96 thi-1 relA1*; Nal^R	(Hanahan 1983)
Top10	F−*mcr*A Δ(*mrr-hsd*RMS-*mcr*BC) Φ80*lacZ*ΔM15 Δ*lac*X74 *rec*A1 *ara*D139 Δ(*ara leu*) 7697 *gal*U *gal*K *rps*L (StrR) *end*A1 *nup*G	Invitrogen
HB101	*supE44 hsdS20 recA13 ara-14 proA2 lacY1 galK2 rpsL20 xyl-5 mtl-1*	(Boyer & Roulland-Dussoix 1969)
CC118λ*pir*	Host strain for pKNG101 replication; Δ(*ara-leu*) *araD* Δ*lacX74 galE galK-phoA20 thi-1 rpsE rpoB argE recA1*, lysogenized with λ*pir*; Rif^R	(Herrero et al. 1990)
P. putida		
KT2440R	Wild-type strain ; Rif^R	(Espinosa-Urgel et al. 2000)
tssA1-Tn5	KT2440R carrying a miniTn5-Km in the *tssA1* (PP3088) gene; Rif^R, Km^R	(Molina-Henares et al. 2010) and this work
tssL1-Tn5	KT2440R carrying a miniTn5-Km in the *tssL1* (PP3092) gene; Rif^R, Km^R	(Molina-Henares et al. 2010) and this work
tssK1-Tn5	KT2440R carrying a miniTn5-Km in the *tssK1* (PP3093) gene; Rif^R, Km^R	(Molina-Henares et al. 2010) and this work
tssG1-Tn5	KT2440R carrying a miniTn5-Km in the *tssG1* (PP3096) gene; Rif^R, Km^R	(Molina-Henares et al. 2010) and this work
tssF1-Tn5	KT2440R carrying a miniTn5-Km in the *tssF1* (PP3097) gene; Rif^R, Km^R	(Molina-Henares et al. 2010) and this work
tssE1-Tn5	KT2440R carrying a miniTn5-Km in the *tssE1* (PP3098) gene; Rif^R, Km^R	(Molina-Henares et al. 2010) and this work
Δ*tssA1*	Markerless KT2440R null mutant in the *tssA1* (PP3088) gene, disabling the K1-T6SS; Rif^R	This work
Δ*tssA1*Δ*tssM2*Δ*tssM3* (ΔT6SS)	Markerless KT2440R null mutant in the *tssA1/tssM2/tssM3*	This work

	(PP3088/PP4071/PP2627) genes disabling all three T6SS clusters; Rif^R	
miniCTX-*hcp1*-HA	KT2440R containing a miniCTX transposon expressing a HA tagged *hcp1* gene; Rif^R, Tc^R	This work
Δ*tssA1* miniCTX-*hcp1*-HA	*tssA1* null mutant containing a miniCTX transposon expressing a HA tagged *hcp1* gene; Rif^R, Tc^R	This work
rpoN::Km	KT2440R carrying a Km cassette in the *rpoN* (PP0952) gene; Km^R	(Köhler et al. 1989)
rpoN::Km *tke2*-V5	*rpoN*::Km mutant in which the *tke2* gene has been replaced by a version tagged with a dual V5 epitope; Km^R	This work
rpoN::Km Δ*tssA1 tke2*-V5	*rpoN*::Km *tke2*-V5 containing the Δ*tssA1* mutation; Km^R	This work
Other strains		
Xanthomonas campestris pv. campestris IVIA 2734-1	Wild-type strain	María Milagros Lopez collection (IVIA, Spain)
Agrobacterium tumefaciens C58	Wild-type strain	Erh Min Lai collection (Academia Sinica, Taiwan)
Pectobacterium carotovorum subsp. carotovorum SCRI 194	Wild-type strain	María Milagros Lopez collection (IVIA, Spain)
Pseudomonas syringae pv tomato DC3000	Wild-type strain	Martin Buck collection (Imperial College London, UK)
Plasmids		
pCR-BluntII-TOPO	Blunt cloning vector; Ap^R, Km^R	Invitrogen
pRK600	Helper plasmid; *ori*ColE1 *mob*RK2 *tra*RK2; Cm^R	(Kessler et al. 1992)
pRK2013	Helper plasmid; *ori*ColE1 *mob*RK2 *tra*RK2; Km^R	(Figurski & Helinski 1979)
pKNG101	Gene replacement suicide vector, *ori*R6K, *oriT*RK2, *sacB;* Sm^R	(Kaniga et al. 1991)
pBAD33	Cloning vector containing the pBAD promoter inducible by L-	(Guzman et al. 1995)

	arabinose; p15A origin; Cm^R	
pNDM220	Low copy number cloning vector containing the *lacI*^{q} gene and the $LacI^q$-regulated promoter PA1/O4/O3, IPTG-inducible; Ap^R	(Gotfredsen & Gerdes 1998)
miniCTX-1	Plasmid for the integration of genes into the *att* site of the *P. putida* chromosome; Tc^R	(Hoang et al. 2000)
pRL662-gfp2	Broad host range vector derived from pBBR1MCS-2 expressing a green fluorescence protein (gfp); Gm^R	Erh-Min Lai collection
pTki2	pBAD33 carrying in SacI-XbaI a 550 bps PCR fragment containing the entire *P. putida tki2* (PP3108.1) gene; Cm^R	This work
pTke2-CT	pNDM220 carrying in BamHI-XhoI a 514 bps PCR fragment containing the C-terminal part of the *P. putida tke2* (PP3108) gene; Ap^R	This work
pK*tssA1*	pKNG101 carrying in XbaI-BamHI a 1.7-Kb PCR fragment containing the regions up- and downstream the *P. putida tssA1* (PP3088) gene; Sm^R	This work
pK*tssM2*	pKNG101 carrying in XbaI-BamHI a 1.6-Kb PCR fragment containing the regions up- and downstream the *P. putida tssM2* (PP4071) gene; Sm^R	This work
pK*tssM3*	pKNG101 carrying in XbaI-BamHI a 1.6-Kb PCR fragment containing the regions up- and downstream the *P. putida tssM3* (PP2627) gene; Sm^R	This work
pK*tke2V5*	pKNG101 carrying in XbaI-BamHI a 1.2-Kb PCR fragment containing a C-terminally V5 dual-tagged *P. putida tke2* gene and the regions up- and downstream this gene; Sm^R	This work
miniCTX-*Plac-hcp1*-HA	miniCTX-1 carrying in EcoRI-BamHI a 0.6-Kb PCR fragment encoding a C-terminal HA-tagged *hcp1* gene from a P*lac* promoter ; Tc^R	This work

[a] Ap^R, Gm^R, Km^R, Nal^R, Rif^R, Sm^R and Tc^R, resistance to ampicillin, gentamycin, kanamycin, nalidixic acid, rifampicin, streptomycin and tetracycline, respectively

References

Boyer HW, Roulland-Dussoix D. (1969). A complementation analysis of the restriction and modification of DNA in Escherichia coli. J. Mol. Biol. 41:459–72.

Espinosa-Urgel M, Salido A, Ramos JL. (2000). Genetic analysis of functions involved in adhesion of Pseudomonas putida to seeds. J. Bacteriol. 182:2363–9.

Figurski DH, Helinski DR. (1979). Replication of an origin-containing derivative of plasmid RK2 dependent on a plasmid function provided in trans. Proc. Natl. Acad. Sci. U.S.A. 76:1648–52.

Gotfredsen M, Gerdes K. (1998). The Escherichia coli relBE genes belong to a new toxin-antitoxin gene family. Mol. Microbiol. 29:1065–76.

Guzman LM, Belin D, Carson MJ, Beckwith J. (1995). Tight regulation, modulation, and high-level expression by vectors containing the arabinose PBAD promoter. J. Bacteriol. 177:4121–30.

Hanahan D. (1983). Studies on transformation of Escherichia coli with plasmids. Journal of molecular biology 166:557–80.

Herrero M, de Lorenzo V, Timmis KN. (1990). Transposon vectors containing non-antibiotic resistance selection markers for cloning and stable chromosomal insertion of foreign genes in gram-negative bacteria. J. Bacteriol. 172:6557–67.

Hoang TT, Kutchma AJ, Becher A, Schweizer HP. (2000). Integration-proficient plasmids for Pseudomonas aeruginosa: site-specific integration and use for engineering of reporter and expression strains. Plasmid 43:59–72.

Kaniga K, Delor I, Cornelis GR. (1991). A wide-host-range suicide vector for improving reverse genetics in gram-negative bacteria: inactivation of the blaA gene of Yersinia enterocolitica. Gene 109:137–41.

Kessler B, de Lorenzo V, Timmis KN. (1992). A general system to integrate lacZ fusions into the chromosomes of gram-negative eubacteria: regulation of the Pm promoter of the TOL plasmid studied with all controlling elements in monocopy. Mol. Gen. Genet. 233:293–301.

Köhler T, Harayama S, Ramos JL, Timmis KN. (1989). Involvement of Pseudomonas putida RpoN sigma factor in regulation of various metabolic functions. J. Bacteriol. 171:4326–33.

Molina-Henares MA, de la Torre J, García-Salamanca A, Molina-Henares AJ, Herrera MC, Ramos JL, et al. (2010). Identification of conditionally essential genes for growth of Pseudomonas putida KT2440 on minimal medium through the screening of a genome-wide mutant library. Environ. Microbiol. 12:1468–85.

Table S2: Sequence of the primers used in this work

Amplified/Deleted gene and promoter region from *P. putida* KT2440	Plasmid	Name	Sequence (5' → 3')[a]
PP3088 (*tssA1*)	pK*tssA1*	tssA1-1	GGAA**TCTAGA**CAACAACCGCGAACGCAG
		tssA1-2	CGGCC**GAATTC**CATAGAACACTCTGGACAT
		tssA1-3	GCCGG**GAATTC**TAGGGGCTGCAATAAAAG
		tssA1-4	TCGGTGAACA**GGATCC**AGTC
PP4071 (*tssM2*)	pK*tssM2*	tssM2-1	TAGAG**TCTAGA**GACGCGCCGAGCCATC
		tssM2-2	CTACATGACTTGATTCATCGAGGCTCC
		tssM2-3	ATGAATCAAGTCATGTAGGCAGGAGGC
		tssM2-4	TTCAA**GGATCC**GCGTGAACGCTCGTTACA
PP2627 (*tssM3*)	pK*tssM3*	tssM3-1	AGGAA**TCTAGA**ACGACGCTACCGGCTACC
		tssM3-2	TCATAGTCGTTGATTCATCGAGGCTCC
		tssM3-3	ATGAATCAACGACTATGAACCTCGTCA
		tssM3-4	ACCTT**GGATCC**TGAGCTGACGCTGCACAT
PP3108 (*tke2*)	pK*tke2V5*	tke2V5-1	GGTCC**TCTAGA**AGAATCTGCGCTTCCAAGGT
		tke2V5-2	aggcttacccgtagaatcgagaccgaggagagggttagggataggcttaccCCATACATCAACTCCTTTAATTACT
		tke2V5-3	gattctacgggtaagcctatccctaaccctctcctcggtctcgattctacgTGAATTAAAGGAGTTGATGTATGG

		tke2V5-4	AATAA**GGATCC**CGGACACCTGCAAAATAC
PP3108 (*tke2*)	pTke2-CT	Tke2-F	CCGGC**GGATCC**taacaggaggaattaaccATGCGTTATGTCACTCAGGACC
		Tke2-R	CCGGG**CTCGAG**CTAcgtagaatcgagaccgaggagagggttagggataggcttaccCCATACATCAACTCCTTTAATTAC
PP3108.1 (*tki2*)	pTki2	Tki2-F	CCGCC**GAGCTC**taacaggaggaattaaccATGGTAATCAATGGCGGTTCATTGG
		Tki2-R	AATTA**TCTAGA**ttagcacgcgtagtccggcacgtcgtacgggtaAGCCCCAAGACCTGTCAACTTGAT
PP3089 (*hcp1*-HA)[b]	miniCTX-*Plac-hcp1*-HA	Hcp1HA-F	CCGCC**GAATTC**taacaggaggaattaaccATGTTGTTAATGGAGAGTTT
		Hcp1HA-R	AACTT**GGATCC**TTAGCACGCGTAGTCCGGCACGTC

[a] The sequences of the restriction sites are indicated in bold and the annealing region is underlined. Artificial Shine-Dalgarno and V5-tag are shown in lowercase.

[b] The strain used as a template for this PCR reaction contains the gene encoding Hcp1 with a C-terminal HA-tag.

Table S3: Distribution of T6SS loci in *Pseudomonas putida strains*

P. putida strain	T6SS clusters	Group 1.1	Group 1.2	Group 2	Group 3	Group 4A	Group 4B	Group 5	VgrGs	Hcps
PA14H7	4		1	2	1				7	3
TRO1	3		1,Partial	1			1		4	2
KT2440	3		2 (K2, K3)				1 (K1)		5	6
DOT-T1E	3		2				1		5	2
H	3		2				1		4	5
LS46	3		2				1		5	3
B6-2	3		2				1		4	3
GB-1	2		1				1		4	5
F1	2		1				1		3	2
ND6	2		1				1		3	3
S13.1.2	2		1				1		4	2
SJTE-1	2		1				1		2	2
str. Idaho	2		1				1		5	3
YKD221	2		1				1		3	2
791_PPUT	2		1				1		5	2
T2-2	2		1				1		3	5
W619	2			1			1		3	4
CBB5	2			1			1		5	2
SQ1	2			1			1		4	4
CSV86	2		1			1			9	3
W15Oct28	2		1	1					6	2
S16	1						1		3	3
NBRC 14164	1						1		3	2
HB3267	1		Partial				1		3	6
DLL-E4	1						1		3	3
PD1	1						1		1	3
SF1	1		Partial				1		5	3
LF54	1						1		3	2
ATH-43	1						1		1	2
UASWS0946	1	1							3	1
S12	1		1						1	1
B001	1		1						2	1
SJ3	1		1						4	1
S610	1		1						2	1
MC4-5222	1			1					7	1
KG-4	1				1				2	1
MTCC 5279	1							1	2	0
BIRD-1	0		Partial						0	0
H8234	0								2	0

Table S4: Characteristics of proteins encoded by the *P. putida* KT2440 K1-T6SS cluster.

Locus name	Protein name	Identities with T6SS PAO1/Other identities	Conserved Domains COG/pfam/TIGR (Short Name)/Phyre (P)[a]	Molecular weight (KDa)/pI[b]	Predicted cellular location[c, d]	Transmembrane Helices[e]	Predicted signal peptide[f, g]
Structural operon							
PP3088	TssA1	PA0082 (HsiA1) 72/316 (23%)	COG3515/pfam06812 (ImpA-rel_N) + TIGR03363 (VI_chp_8)	361 a.a. 39.9/4.4	1. Unknown 2. Cytoplasmic	0	No Yes (1-18)
PP3089	TssD1/Hcp1	PA0085 (Hcp1) 53/169 (31%)	COG3157 (Hcp)/ pfam05638 (DUF796)/ TIGR03344 (VI_effect_Hcp1)	180 a.a. 19.5/5.3	1. Extracellular 2. Cytoplasmic	0	No No
PP3090	TagP1	PA0077 (IcmF1) 151/406 (37%)	COG3523 (IcmF)/ pfam14331 (ImcF-related_N)/TIGR03348 (VI_IcmF) + pfam00691 (OmpA)	831 a.a. 93.1/9	1. Inner Membrane 2. Inner Membrane	3	No No
PP3090.1	TagF1	PA0076 (TagF1) 8/22 (36%)	pfam (DUF2094)	302 a.a. 33.8/6.2	1. Cytoplasmic 2. Unknown	0	No No
PP3091	TssM1	PA0077 (IcmF1) 152/466 (33%)	COG3523 (IcmF)/ pfam14331 (ImcF-related_N)/TIGR03348 (VI_IcmF)	1267 a.a. 138.7/6.8	1. Inner Membrane 2. Inner Membrane	3	No No
PP3092	TssL1	PA0078 (TssL1) 50/187 (27%)	COG3455/pfam09850 (DUF2077)/ TIGR03349 (TIGR03349)	238 a.a. 26.9/5.7	1. Cytoplasmic 2. Inner Membrane	1	No No
PP3093	TssK1	PA0079 (TssK1) 140/450 (31%)	COG3522/ pfam05936 (DUF876)/TIGR03353 (VI_chp_4)	447 a.a. 50/6.4	1. Cytoplasmic 2. Unknown	0	No No
PP3094	TssJ1	PA0080 (TssJ1) 33/107 (31%)	COG3521/pfam12790 (T6SS-SciN)/TIGR03352 (VI_chp_3)	240 a.a. 25.9/4.7	1. Unknown 2. Periplasm	0	No Yes (1-26)
PP3095	TssH1/ ClpV1	PA0090 (ClpV1) 452/893 (51%)	COG0542 (ClpA) + pfam07724 (AAA_2)/ TIGR03345 (VI_ClpV1)	878 a.a. 96.5/6.1	1. Cytoplasmic 2. Unknown	0	No Yes (1-22)
PP3096	TssG1	PA0089 (TssG1) 111/328 (34%)	COG3520/pfam06996 (DUF1305)/TIGR03347 (VI_chp_1)	356 a.a. 40.8/9.9	1. Cytoplasmic 2. Cytoplasmic	0	No No
PP3097	TssF1	PA0088 (TssF1) 216/632 (34%)	COG3519/pfam05947 (DUF879)/TIGR03359 (VI_chp_6)	606 a.a. 69.2/7.3	1. Cytoplasmic 2. Cytoplasmic	0	No No
PP3098	TssE1	PA0087 (TssE1) 42/138 (30%)	COG3518/ pfam04965 (GPW_gp25)/ TIGR03357 (VI_zyme)	160 a.a. 18.4/8.5	1. Cytoplasmic 2. Cytoplasmic	0	No No
PP3099	TssC1	PA0084 (TssC1) 251/486 (52%)	COG3517/pfam05943 (DUF877)/TIGR03355 (VI_chp_2)	500 a.a. 56.1/4.9	1. Cytoplasmic 2. Cytoplasmic	0	No No
PP3100	TssB1	PA0083 (TssB1) 68/161 (42%)	COG3516/pfam05591 (DUF770)/TIGR03358 (VI_chp_5)	191 a.a. 21.7/7.7	1. Cytoplasmic 2. Cytoplasmic	0	No No
PP3100.1	TagX1		--	254 a.a. 28.5/5.5	1. Cytoplasmic 2. Unknown	0	No No
Intermediate region							
PP3100.2			--	68 a.a. 7.15/9.26	1. Unknown 2. Periplasm	0	No No
PP3100.3			--	183 a.a. 20.6/9.04	1. Inner Membrane	3	No Yes (1-40)

					2. Inner Membrane		
PP3101			COG1397 (DraG)/ pfam03747 (ADP_ribosyl_G)/ TIGR02662 (dinitro_DRAG)	260 a.a. 28.7/6.5	1. Unknown 2. Unknown	0	No No
PP3101.1			--	90 a.a. 10.2/4.81	1. Unknown 2. Cytoplasmic	0	No No
PP3101.2			--	189 a.a. 21.5/10.7	1. Unknown 2. Cytoplasmic	0	No No
PP3101.3	Partial	PP3106 28/61 (46%)	--	112 a.a. 12.8/9.5	1. Unknown 2. Unknown	0	No No
PP3101.4	Partial	PP3105 100/231 (43%)	--	232 a.a. 26.2/9.94	1. Inner membrane 2. Inner membrane	6	No No
PP3101.5	Partial	PP3106 31/51 (61%)	Pfam05954 (Phage GPD)	67 a.a. 7.6/9.30	1. Unknown 2. Cytoplasmic	0	No No
PP3101.6	Partial		COG0013: Alanyl-tRNA synthetase	103 a.a. 11.9/5.9	1. Unknown 2. Cytoplasmic	0	No No
PP3101.7			--	101 a.a. 11.1/6.31	1. Unknown 2. Cytoplasmic	0	No No
PP3101.8	Partial		COG3344/ pfam00078/ TIGR04416/ (RVT_1) Group II intron reverse transcriptase	129 a.a. 14.8/10.5	1. Unknown 2. Cytoplasmic	0	No No
PP3101.9	Partial		Ribosomal protein S7 cl00313:uS7 Superfamily	58 a.a. 6.7/10.15	1. Unknown 2. Unknown	0	No No
PP3102	Tki1	PA0092 (Tsi6) 44/93 (47%)	P:Tsi6 (4-89 a.a.) C:100%	98 a.a. 10.9/8.4	1. Unknown 2. Cytoplasmic	0	No No
PP3103	Tke1	PA0093 (Tse6) 88/160 (55%)	pfam (Toxin_61) P: Tse6 (227-383 a.a.) C: 100%	391 a.a. 42.6/9.9	1. Unknown 2. Inner Membrane	0	No No
PP3103.1			--	98 a.a. 11.5/9.1	1. Unknown 2. Inner Membrane	1	No No
VgrG1 operon							
PP3104			--	338 a.a. 35.1/9.5	1. Unknown 2. Inner Membrane	1	No No
PP3105		PP3101.4 100/231 (43%)	--	231 a.a. 26.5/10.5	1. Inner Membrane 2. Inner Membrane	4	No No
PP3106	TssI1/VgrG1	PA0091 (VgrG1) 213/588 (36%)	COG3501 (VgrG)/ pfam05954 (Phage_GPD)/ TIGR03361 (VI_Rhs_Vgr)	618 a.a. 69.5/5.6	1. Cytoplasmic 2. Extracellular	0	No No
PP3106.1	EagR1a	PA0094 6/14 (43%)	pfam08786 (DUF1795)	194 a.a. 21.6/5.8	1. Cytoplasmic 2. Unknown	0	No No
PP3107	EagR1b	PA0094 39/141 (28%)	COG5435/pfam08786 (DUF1795)	173 a.a. 19.1/4.9	1. Unknown 2. Extracellular	0	No No
PP3108	Tke2		pfam05488 (PAAR_motif) + COG3209 (RhsA)/ TIGR03696 (Rhs_assc_core) + HNH nuclease (SM00507) / P: Endonuclease (1331-1362 a.a.) C: 50%	1385 a.a. 155.8/6	1. Unknown 2. Inner Membrane	2	No No
PP3108.1	Tki2		--	158 a.a. 17.4/4.6	1. Cytoplasmic 2. Cytoplasmic	0	No No
PP3108.2	Partial	PP3108 207/219 (95%)	pfam05593 (RHS-repeat)	278 a.a. 31.2/5.4	1. Unknown 2. Extracellular	0	No No

PP3108.3			pfam14136 (DUF4303)	176 a.a. 20.4/4.5	1. Unknown 2. Cytoplasmic	0	No No
PP3109	Partial	PP3108 24/26 (92%)	pfam03527 (RHS)	143 a.a. 16.1/11.1	1. Inner Membrane 2. Inner Membrane	1	No No
PP3109.1			P: Multiheme cytochromes (28-120 a.a.) C: 65%	159 a.a. 18.2/5.1	1. Cytoplasmic 2. Cytoplasmic	0	No No
PP3109.2	Partial		pfam14427 (Pput2613-deam)	76 a.a. 8.1/5.8	1. Unknown 2. Cytoplasmic	0	No No
PP3109.3	Partial		Pfam15588 (Imm7)	75 a.a. 8/4.1	1. Unknown 2. Cytoplasmic	0	No No
PP3109.4	Tke3		P: B30.2 domain of TRIM20 (103-198 a.a.) C: 84%	199 a.a. 22.3/5.2	1. Cytoplasmic 2. Unknown	0	No No
PP3109.5	Tki3		Pfam15428 (Imm14)	173 a.a. 20/8.3	1. Cytoplasmic 2. Cytoplasmic	0	No No
PP3109.7			--	201 a.a. 23.2/6.3	1. Cytoplasmic 2. Outer membrane	0	No No
PP3110			--	70 a.a. 8/10	1. Unknown 2. Periplasm	0	No No
PP3111			Pfam09339 (HTH-IclR)	34 a.a. 3.7/7.6	1. Unknown 2. Unknown	0	No No

a.a.: amino acids
Newly annotated proteins are in bold
Partial proteins or those with premature stop codon are underline

a: Structural-based homology prediction using the Protein Homology/analogy Recognition Engine (Phyre) server (Kelley, et al., 2009). C stands for Confidence.
b: The molecular weight and isoelectric point (pI) are based on prediction by the software ExPASy (http://www.expasy.ch/tools/pi_tool.html).
c: The cellular localization is based on prediction by PSORTb (http://www.psort.org/psortb/index.html).
d: The cellular localization is based on prediction by SOSUIGramN (http://bp.nuap.nagoya-u.ac.jp/sosui/sosuigramn/sosuigramn_submit.html).
e: The prediction of transmembrane domains was determined by TMHMN (http://www.cbs.dtu.dk/services/TMHMM/)
f: The prediction of signal peptides was determined by SignalP (http://www.cbs.dtu.dk/services/SignalP/).
g: The prediction of signal peptides was determined by SOSUIsignal (http://bp.nuap.nagoya-u.ac.jp/sosui/sosuisignal/sosuisignal_submit.html).

Table S5: Characteristics of proteins encoded by the *P. putida* KT2440 K2- and K3-T6SS clusters

Locus name	Protein name	Protein length	Identities with H2-T6SS PAO1	K2-K3 Identities /Other identities	Conserved Domains COG/pfam/TIGR (Short Name)/ Phyre[a]	Predicted cellular location[b, c]	Transmem-brane helices[d]	Predicted signal peptide[e, f]
PP4071	TssM2	1208 a.a.	PA1669 (IcmF2) 26%	82%	COG3523 (IcmF) pfam06761(IcmF) TIGR03348 (VI_IcmF)	1. Inner Membrane 2. Inner Membrane	3	No No
PP2627	TssM3	1206 a.a.	27%					
PP4072	TssA2	488 a.a.	PA1656 (HsiA2) 26%	77%	pfam06812 (ImpA-rel_N)+ TIGR03362 (VI_chp_7)	1. Cytoplasmic 2. Cytoplasmic	0	No No
PP2626	TssA3	487 a.a.	24%			1. Cytoplasmic 2. Inner Membrane		
PP4073	VasI2	210 a.a.		64%	Pfam11319 (DUF3121)/ TIGR03360 (VI_minor_1)	1. Cytoplasmic 2. Unknown	0	No Yes (1-23)
PP2625	VasI3	231 a.a.				1. Cytoplasmic 2. Cytoplasmic	1	No No
PP4074	TssB2	167 a.a.	PA1657 (HsiB2) 50%	82%	COG3516/pfam05591(DUF770)/TIGR03358 (VI_chp_5)	1. Cytoplasmic 2. Cytoplasmic	0	No No
PP2624	TssB3	167 a.a.	50%					
PP4075	TssC2 (partial)	428/495*a.a.	PA1658 (HsiC2) 65%	84%	COG3517/ pfam05943 (DUF877)/ TIGR03355 (VI_chp_2)	1. Cytoplasmic 2. Cytoplasmic	0	No No
PP2623	TssC3	496 a.a.	67%					
PP4076	TssE2	136 a.a.	PA1659 (HsiF) 27%	88%	COG3518/ pfam04965 (GPW_gp25)/ TIGR03357 (VI_zyme)	1. Cytoplasmic 2. Unknown	0	No No
PP2622	TssE3	136 a.a.	30%					
PP4077	TssF2	588 a.a.	PA1660 (HsiG) 35%	86%	COG3519/ pfam05947 (DUF879)/ TIGR03359 (VI_chp_6)	1. Cytoplasmic 2. Cytoplasmic	0	No No
PP2621	TssF3	588 a.a.	34%					
PP4078	TssG2	338 a.a.	PA1661 (HsiH) 34%	88%	COG3520/ pfam06996 (DUF1305)/ TIGR03347 (VI_chp_1)	1. Cytoplasmic 2. Cytoplasmic	0	No No
PP2620	TssG3	338 a.a.	35%			1. Unknown 2. Cytoplasmic		
PP2619	Fha3	189 a.a.	PA1665 (Fha2) 25%		COG3456/TIGR03354 (VI_FHA)	1. Unknown 2. Cytoplasmic	0	No No
PP4079	TssJ2	265 a.a.	PA1666 (Lip2) 22%	76%	COG3521/pfam12790 (T6SS-SciN)/TIGR03352 (VI_chp_3)	1. Unknown 2. Periplasm	0	No Yes (1-27)
PP2618	TssJ3	265 a.a.	27%					Yes (1-23) Yes (1-23)
PP4080	TssK2	445 a.a.	PA1667 (HsiJ2) 35%	91%	COG3522/pfam05936 (DUF876)/ TIGR03353 (VI_chp_4)	1. Cytoplasmic 2. Periplasm	0	No No
PP2617	TssK3	445 a.a.	35%					
PP4081	TssL2	310 a.a.	PP1668(DotU2) 34%	85%	COG3455/ pfam09850 (DUF2077)/ TIGR03349 (IV_VI_DotU)	1. Unknown 2. Inner Membrane	1	No No
PP2616	TssL3	289 a.a.	34%					
PP4082	TssD2/Hcp2	171 a.a.	PA1512 (Hcp2) 58%	99%	COG3157 (Hcp)/ pfam05638 (DUF796)/ TIGR03344 (VI_effect_Hcp1)	1. Extracellular 2. Extracellular	0	No No
PP2615	TssD3/Hcp3	171 a.a.	58%					

PP4083	TssI2/VgrG 2 (partial)	361/659 a.a.	PA1511 (VgrG2a) 49%	76%	COG3501 (VgrG)/ pfam05954 (Phage_GPD)/ TIGR03361 (VI_Rhs_Vgr)	1. Cytoplasmic 2. Cytoplasmic	0	No No
PP2614	TssI3/VgrG 3	722 a.a.	53%					

PP2613	Fha3	316 a.a.			pfam13503 (DUF4123)	1. Unknown 2. Cytoplasmic	0	No No
PP2612	Tke5	996 a.a.			--	1. Inner Membrane 2. Unknown	5	No Yes (1-35)
PP2611	Tki5	319 a.a.			pfam11746 (DUF3303)	1. Inner Membrane 2. Inner Membrane	4	No Yes (1-21)
PP2610	Tsp5	85 a.a.			COG4101/pfam05488 (PAAR_motif)	1. Unknown 2. Cytoplasmic	0	No No

PP4084	EagR2	143 a.a.			COG5435/ pfam08786 (DUF1795)	1. Unknown 2. Cytoplasmic	0	No No
PP4085	Tke4	1530 a.a.			Pfam05488 (PAAR_motif) + COG3209(RhsA)/ pfam03527(RHS)/ TIGR03696 (Rhs_assc_core) + pfam15652 (Tox-SHH)	1. Unknown 2. Inner Membrane	3	No Yes (1-28)
PP4085.1	Tki4	161 a.a.		PP4094 96%	SM000860(SMI1/ KNR4 family) Imm-SUKH	1. Unknown 2. Extracellular	0	No No
PP4085.2		143 a.a.		PP4094.1 73%	--	1. Cytoplasmic 2. Cytoplasmic	0	No No
PP4086		187 a.a.			--	1. Inner Membrane 2. Cytoplasmic	1	No No
PP4087		50 a.a.			--	1.Unknown 2. Unknown	0	No No
PP4087.1	Partial	100 a.a.			TIGR03696 (Rhs_assc_core)	1. Unknown 2. Cytoplasmic	0	No No
PP4087.2	Partial	140 a.a.			pfam15428 (Imm14)	1. Unknown 2. Cytoplasmic	0	No No
PP4088	Partial	491a.a.		PP4085 95%	pfam05593 (RHS_repeat)	1. Unknown 2. Extracellular	0	No No
PP4089	Partial	422 a.a.		PP4085 82%	pfam03257 (RHS)	1. Unknown 2. Extracellular	0	No No
PP4089.1		153 a.a.			--	1.Cytoplasmic 2. Cytoplasmic	0	No No
PP4090	Partial	302 a.a.		PP4085 98%	pfam05593 (RHS_repeat)	1. Unknown 2. Extracellular	0	No No
PP4091	ISPpu15 Orf2				COG3436/ pfam03050 (DDE_Tnp_IS66)			
PP4092	ISPpu15 Orf1				COG3436/ pfam05717 (TnpB_IS66)			
PP4093	Partial	198 a.a.		PP4085 57%	COG3209 (RhsA)/TIGR03696 (tRNA_nuclease_WapA)	1. Unknown 2. Cytoplasmic	0	No No
PP4093.1	Partial	212 a.a.			P: Hypothetical protein YwqG (pdb: d1pv5a) (143-212 a.a.) C: 93%	1. Unknown 2. Outer Membrane	0	No No
PP4094	Tki4b	161 a.a.		PP4085.1 96%	SM000860(SMI1/ KNR4 family) Imm-SUKH	1. Cytoplasmic 2. Extracellular	0	No No
PP4094.1		101 a.a.		PP4085.2	Pfam09827	1. Unknown	0	No

				73%	(CRISPR_Cas2)	2. Cytoplasmic		No
PP4095	Partial	91 a.a.			pfam05954 (Phage GPD)	1. Unknown 2. Cytoplasmic	0	No No

a.a.: amino acids.
Newly annotated proteins are in bold
Partial proteins or those with premature stop codon are underline

a: Structural-based homology prediction using the Protein Homology/analogy Recognition Engine (Phyre) server (Kelley, et al., 2009). C stands for Confidence.
b: The cellular localization is based on prediction by PSORTb (http://www.psort.org/psortb/index.html).
c: The cellular localization is based on prediction by SOSUI GramN (http://bp.nuap.nagoya-u.ac.jp/sosui/sosuigramn/sosuigramn_submit.html).
d: The prediction of transmembrane domains was determined by TMHMN (http://www.cbs.dtu.dk/services/TMHMM/)
e: The prediction of signal peptides was by SignalP (http://www.cbs.dtu.dk/services/SignalP/).
f: The prediction of signal peptides was by SOSUIsignal (http://bp.nuap.nagoya-u.ac.jp/sosui/sosuisignal/sosuisignal_submit.html).

Table S6: Characteristics of proteins encoded by orphan *hcp* and *vgrG* gene clusters

Locus name	Gene name Protein name	Identities	Conserved Domains COG/pfam/TIGR (Short Name)/Phyre[a]	Molecular weight (KDa)/pI[b]	Predicted cellular location[c, d]	Transmembrane helices[e]	Predicted signal peptide[f, g]	Predicted non-classically secreted protein[h]
Orphan Hcp4 cluster								
PP0646	Tke6		COG4101/pfam05488 (PAAR_motif) + P: Colicin n (242-460 a.a.) C: 87.6%	466 a.a. 48.7/5.8	1. Unknown 2. Inner membrane	2	No No	No
PP0647	Tki6		--	129 a.a. 14.6/9.46	1. Inner membrane 2. Inner membrane	3	No Yes (1-37)	No
PP0655	Hcp4 (Partial)	PA0085 (Hcp1) 24/80 (30%)	COG3157/pfam05638 (DUF796)	108 a.a. 11.7/4.2	1. Unknown 2. Extracellular	0	No No	Yes
Orphan Hcp5 cluster								
PP4884.1	Tki7	PP5238.2 43/ 104 (41%)	--	124 a.a. 14.3/10.3	1. Inner membrane 2. Inner membrane	2	No No	No
PP4885	Tke7	PP5238.1 152/250 (61%)	P: Colicin s4 (57-314 a.a.) C: 95%	323 a.a. 34/6.4	1. Cytoplasmic 2. Unknown	0	No No	No
PP4886	Hcp5	PA0085 (Hcp1) 47/157 (30%) PP5238 (Hcp6) 150/162 (93%)	COG3157/pfam05638 (DUF796)/TIGR03344 (VI_effect_Hcp1)	181 a.a. 19.8/8.4	1. Extracellular 2. Unknown	0	No No	Yes
Orphan Hcp6 cluster								
PP5238	Hcp6	PA0085 (Hcp1) 47/157 (30%) PP4886 (Hcp5) 150/162 (93%)	COG3157/pfam05638 (DUF796)/TIGR03344 (VI_effect_Hcp1)	162 a.a. 17.5/7.2	1. Extracellular 2. Cytoplasmic	0	No No	Yes
PP5238.1	Tke8	PP4885 (Tke7) 152/250 (61%)	P: Colicin n (43-258 a.a.) C: 68%	260 a.a. 26.9/7.8	1. Cytoplasmic 2. Inner membrane	0	No No	No
PP5238.2	Tki8	PP4884.1 (Tki7) 43/104 (41%)	--	149 a.a. 17/9.3	1. Inner membrane 2. Inner membrane	3	No No	No
Orphan VgrG4 cluster								
PP3385	TssL4	PA1668 (DotU2) 69/207 (33%)	COG3455/pfam09850 (DUF2077)/TIGR03349 (IV_VI_DotU)	282 a.a. 32.4/6	1. Cytoplasmic 2. Inner membrane	1	No No	No
PP3386	VgrG4	PA1511 (VgrG2a) 270/506 (53%)	COG3501 (VgrG)/ pfam05954 (Phage_GPD)/ TIGR03361 (VI_Rhs_Vgr)	725 a.a. 82/6.1	1. Cytoplasmic 2. Cytoplasmic	0	No No	No
PP3387	Tap4	PA1854 38/134 (28%)	pfam13503 (DUF4123)	315 a.a. 34.9/7.7	1. Unknown 2. Cytoplasmic	0	No No	No
PP3388	Tke9		--	890 a.a. 99.2/6.8	1. Unknown 2. Inner membrane	2	No No	No
PP3389	Tki9		--	385 a.a.	1. Inner	3	No	No

				43.3/10.4	membrane 2. Inner membrane		No	

Orphan VgrG5 cluster								
PP4045	Tsp10	PA0093 (Tke6) 18/46 (39%)	COG4104/pfam05488 (PAAR_motif)	88 a.a. 8.9/6	1. Unknown 2. Cytoplasmic	0	No Yes (1-13)	Yes
PP4046	Tki10b	PA2201 35/143 (24%) PP4047 (Tki10a) 120/320 (38%)	pfam08928 (DUF1910) Imm PA2201	320 a.a. 37.1/6.5	1. Cytoplasmic 2. Cytoplasmic	0	No No	No
PP4047	Tki10a	PA2201 44/152 (29%) PP4046 (Tki10b) 120/320 (38%)	pfam08929 (DUF1911) Imm PA2201	318 a.a. 37.1/5.3	1. Cytoplasmic 2. Cytoplasmic	0	No No	No
PP4048	Tke10		Tox-REase-1 (Zhang et al. 2012)	507 a.a. 54.8/8.5	1. Unknown 2. Inner Membrane	1	No No	No
PP4049	VgrG5	PA1511 (VgrG2a) 259/509 (51%)	COG3501 (VgrG)/ pfam05954 (Phage_GPD)/ TIGR03361 (VI_Rhs_Vgr)	771 a.a. 85.6/6	1. Cytoplasmic 2. Cytoplasmic	0	No No	No

a.a.: amino acids
Newly annotated proteins are in bold
Partial proteins or those with premature stop codon are underline

a: Structural-based homology prediction using the Protein Homology/analogy Recognition Engine (Phyre) server (Kelley, et al., 2009). C stands for Confidence.
b: The molecular weight and isoelectric point (pI) are based on prediction by the software ExPASy (http://www.expasy.ch/tools/pi_tool.html).
c: The cellular localization is based on prediction by PSORTb (http://www.psort.org/psortb/index.html).
d: The cellular localization is based on prediction by SOSUIGramN (http://bp.nuap.nagoya-u.ac.jp/sosui/sosuigramn/sosuigramn_submit.html).
e: The prediction of transmembrane domains was determined by TMHMN (http://www.cbs.dtu.dk/services/TMHMM/)
f: The prediction of signal peptides was by use of SignalP (http://www.cbs.dtu.dk/services/SignalP/).
g: The prediction of signal peptides was determined by SOSUIsignal (http://bp.nuap.nagoya-u.ac.jp/sosui/sosuisignal/sosuisignal_submit.html).
h: The prediction was determined by SecretomeP (http://www.cbs.dtu.dk/services/SecretomeP/).